EuCARD

European Coordination for Accelerator Research and Development

Seventh Framework Programme, Capacities Specific Programme, Research Infrastructures, Combination of Collaborative Project and Coordination and Support Action

DELIVERABLE REPORT

STUDY OF IR DESIGN FOR THE LHC UPGRADE

DELIVERABLE: D11.2.2

Document identifier:	EuCARD-Del-D11-2-2-v11
Due date of deliverable:	End of Month 48 (March 2013)
Report release date:	30/07/2013
Work package:	WP11: ANAC
Lead beneficiary:	CERN
Document status:	Final

Abstract:

A conceptual novel optics was developed for a future upgrade of the LHC interaction regions (IR). Applying the collision scheme with a large Piwinski angle and crab waist, originating from e^+e^- colliders, to an existing pp collider requires fairly unequal IP beta functions, while the transverse proton emittances are naturally equal. The extremely small vertical IP beta function calls for a novel final magnetic focusing element, a so-called double half quadrupole. At least a partial local chromatic correction is mandatory. Similar, simpler optics designs were explored for the LHeC electron beam. Possible benefits were also studied for higher-energy proton collisions at the HE-LHC, for which the proposed scheme appears quite attractive. Pertinent beam experiments were performed, analysed and prepared at DAΦNE and LHC.

Delivery Slip

	Name	**Partner**	**Date**
Authored by	J.L. Abelleira	CERN	30/04/2013
Contributors	J.L. Abelleira, O. Dominguez, C. Milardi, S. Russenschuck, D. Shatilov, R. Tomas, F. Zimmermann, M. Zobov	CERN, INFN, BINP	30/04/2013
Reviewed by	F. Zimmermann	CERN	22/05/2013
Approved by WP Coordinator	M.E. Biagini	INFN	06/06/2013
Approved by Project coordinator	Jean-Pierre Koutchouk		22/07/2013

TABLE OF CONTENTS

1.

EXECUTIVE SUMMARY

A novel optics for a possible future luminosity upgrade of the LHC was explored and developed, which combines several new elements, hitherto only considered for e^+e^- colliders (with unequal horizontal and vertical emittances, and beams of opposite charge), such as flat beams, large Piwinski angle, partial local chromatic correction, and the possibility of a crab-waist scheme with sextupoles. In the frame of this work, similar optics designs were also developed for the LHeC and the potential benefit of a similar scheme was explored for the HE-LHC.

This study was motivated by a proposal for the former SuperB project and the subsequent successful demonstration of crab-waist collisions in the DAΦNE collider, with the goal to study its applicability for a pp collider like the LHC.

It included experimental beam tests of the crab-waist scheme in DAΦNE and of collisions with a large Piwinski angle in the LHC, as well as beam-beam simulations of achievable luminosity gains, and the practical preparation of LHC flat beam tests.

Various local and non-local chromatic corrections schemes were initially designed and compared for the conceptually simpler LHeC case with a single low-energy electron beam.

A beam-beam study together with frequency-map analysis was used to identify the beam parameter range for which crab-waist collisions would be beneficial at the LHC, and guided the optics design. In particular the minimum beam flatness σ_x^*/σ_y^* required for a successful crab-waist application was inferred from this study.

For the LHC luminosity upgrade two specific optics configurations were developed and qualified. The first optics features more ambitious beta* values and demands a local chromatic correction in both planes. Its dynamic aperture determined by particle tracking appears insufficient. The second optics is more relaxed and allows for a partial local chromatic correction in the vertical plane only, while the horizontal chromaticity can be controlled with the arc sextupoles. The dynamic aperture is acceptable. This optics therefore represents the proposed solution for the LHC.

A key hardware ingredient of either optics is a novel "double half quadrupole" which focuses either beam in the vertical plane in a common aperture.

Advantages of a similar collision scheme were studied for the HE-LHC, where it profits from a naturally smaller vertical emittance.

2. INTRODUCTION

LHC upgrades are a central theme of EuCARD and also pursued in EuCARD Work Packages 4 (AccNet), 7 (HFM), 8 (ColMat), and 10 (SRF).

An upgrade of the Interaction Region (IR) of the two high-luminosity experiments, ATLAS and CMS should provide these experiments with about a factor 10 higher integrated luminosity than the nominal LHC.

It has also known since 2001/02 that operation with a large Piwinski angle $\phi \gg 1$ decreases the beam-beam effects so that the same tune shift is reached only for much brighter beams, with corresponding increases in total intensity, peak luminosity, beam lifetime and integrated luminosity [1]. The Piwinski angle is defined as $\varphi = \theta_c \sigma_z / (2\sigma_x^*) \gg 1$, where θ_c denotes the crossing angle, σ_z the rms bunch length and σ_x^* the horizontal beam size in the (horizontal) plane of crossing.

In 2006 a novel crab-waist scheme was proposed for the design of the SuperB e^+e^- collider [2]. Less than two years later its merits were experimentally demonstrated at the DAΦNE e^+e^- collider in Frascati [3], where it provided about a factor 3 increase in peak luminosity. The crab waist scheme comes along with a much reduced vertical β-function (β_y^*) and with a large Piwinski angle. In addition to lower beam-beam tune shifts, the advantages of LPA include a reduction in the hourglass effect over the length of the collision thanks to the reduced longitudinal extent of the collision area, which supports a significant β^* decrease.

The goal of the EuCARD WP11.2 study was to study whether this same collision concept could be applied to the LHC. The implementation of a crab-waist collision scheme at the LHC is not straightforward. While DAΦNE and SuperB collide electron and positron beams of opposite charge and with rather unequal transverse emittances, $\varepsilon_x \gg \varepsilon_y$, the LHC proton beams have the same sign of charge and are naturally round ($\varepsilon_x = \varepsilon_y$). However, the crab-waist scheme can be applied only with flat beam sizes at the collision point, e.g. $\sigma_x^* \gg \sigma_y^*$. In the case of the LHC this condition then translates into highly unequal beta functions, $\beta_x^* \gg \beta_y^*$, which favour a symmetric doublet focusing optics rather than the present asymmetric triplet optics and call for a dedicated local chromatic correction at least in the vertical plane.

The combination of flat beams and a large Piwinski angle can alone boost the luminosity of the LHC, but it also is a necessary condition for implementing the crab-waist collision scheme.

A (partial) local chromatic correction scheme is realized by installing chromatic sextupoles near the IP. The optics development proceeded in steps. Several aspects of this new LHC-upgrade optics, including the local chromatic correction, were initially developed and tested for the LHeC, a proposed future electron-proton collider, based on the LHC.

Since a symmetric IR optics is preferred with flat beams, the polarity of half of the final quadrupoles should be different from the present configuration. This requirement also applies to the region where the two beams travel inside the same aperture. As part of the WP11.2 study for this region close to the IP, a novel magnetic element, called the double half quadrupole (DHQ), has been proposed, which would provide quadrupolar fields of opposite sign at opposite locations from the aperture centre. This element helps squeezing the vertical β-function for the two beams to the small value required at the IP.

Finally, we have designed an optics for a proposed future high-energy hadron collider, HE-LHC, where radiation damping becomes so strong that the proton beam emittances become flat, $\varepsilon_x \gg \varepsilon_y$, as for e^+e^- colliders, simplifying the implementation and maximizing the potential benefit.

3. NOVEL ELEMENTS FOR AN LHC LUMINOSITY INCREASE

3.1. LOCAL CHROMATIC CORRECTION

The chromatic correction in the present LHC is realized by sextupole magnets located in the arcs. Thanks to the high value of dispersion in the arc locations the sextupoles can correct the chromaticity generated over the entire ring, including the interaction regions, for the nominal IP beta functions. Attempts to increase the luminosity through a reduction in β* encounters a limit from the chromatic correction scheme. As β* decreases the β-functions in the quadrupoles of the final focus system grow, increasing the overall chromaticity, until the maximum strength of the correcting sextupoles in the arcs is reached, for a β^* of about 30 cm (without the so-called "ATS" optics [4]). On the other hand, when the chromaticity is not locally corrected, intrinsic limitations restrict the momentum bandwidth of the system due to the fact that the phase relations between sextupoles and the final focus system are broken for off-momentum particles A scheme to correct chromaticity locally was proposed in 2001 for linear colliders [5,6]. Here two sextupoles are used to correct chromaticity, one for each plane; and two or three more sextupoles to compensate the geometric aberrations generated by the former two.

3.1.1. Local chromatic correction for LHeC

A local chromatic correction scheme has first been developed for the electron line of the LHeC [Abe01,Abe02,Abe03,Abe04]. Figure 1 displays the optics of the system, where two chromatic sextupoles are in a dispersive region and the other two, the ones that compensate the geometric aberrations, are in a zero dispersion region.
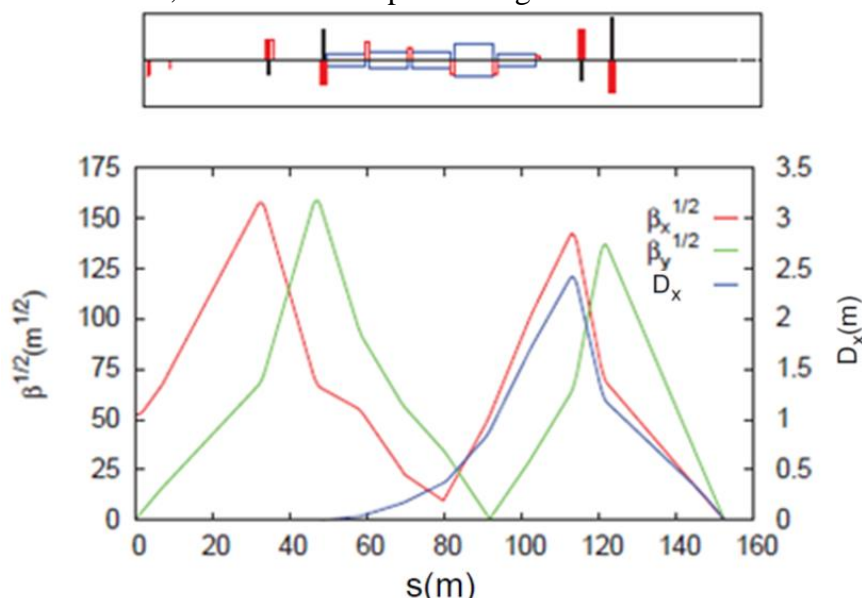
Figure 1: LHeC FF optics with local chromatic correction.

The performance of this final-focus system with local chromatic correction was compared with those for a triplet without chromatic correction and for a traditional chromatic correction final focus. The local approach is more compact and provides a larger bandwidth. However, the horizontal emittance and beam-size increase due to SR emitted in bending magnets is considerably higher, due to the large dispersion in the bending magnets. This beam-size

increase due to synchrotron radiation is reduced by weaker bending magnets and smaller dispersion, which however implies stronger sextupoles and renders the correction of aberrations more difficult. The code MAPCLASS was employed to evaluate the contribution of chromatic and geometric aberrations and to minimize them by optimizing the values for the sextupole strengths and dispersion; see Fig. 2.
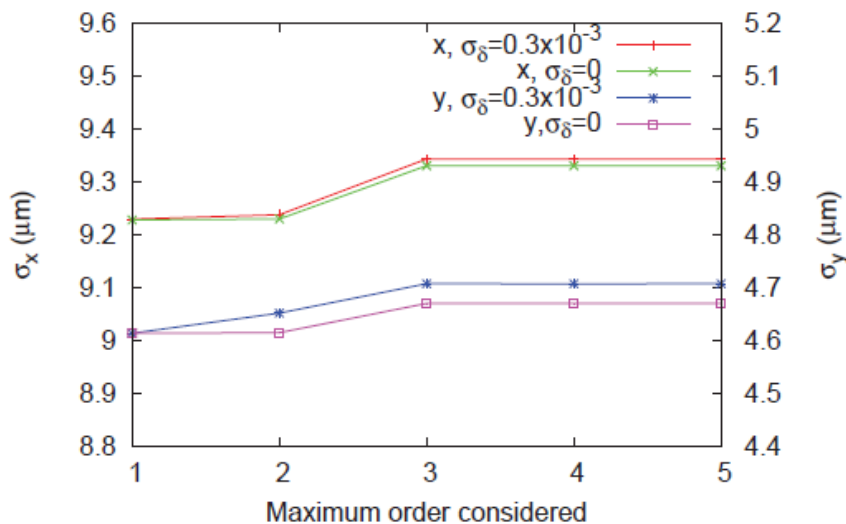

Figure 2: Beam sizes as a function of map order computed with MAPCLASS for the FF with local chromatic correction of Fig. 1, after optimization.

3.1.2. Local chromatic correction for LHC

Several past studies considered the possibility of performing a local chromatic correction in the LHC [7,8,9]. An LHC with local chromatic correction would allow for a lower β* decrease and larger off-momentum dynamic aperture. Local chromatic correction requires sextupole magnets to be installed in the IR as well as significant non-zero dispersion at some of these sextupoles. Ideally, the IR sextupoles would be installed at places where the β-function in one plane is much larger than in the other plane. These conditions are not met for the present LHC final focus scheme, which is based on a triplet.

3.2. FLAT BEAMS

The LHC IRs are designed for beam collisions with equal size in the horizontal and in the vertical plane, a situation which is commonly known as "round beam" collision. For the nominal LHC, β^* has the same value in the two transverse planes. It is difficult to achieve a high ratio of β_x^*/β_y^* with the present final-focus scheme involving triplet focusing.

For a proton machine the normalized emittances are preserved and at the LHC they have the same value in the two planes. This is not the case of lepton colliders, where usually the horizontal emittance is much bigger than the vertical one, which corresponds to the natural equilibrium in the presence of strong synchrotron radiation. These flat beams facilitate the use of unequal β-functions in the two planes, e.g. by equalizing the beam divergence. The unequal β^* easily yields for the final quadrupoles with negative strength (vertically focusing) the possibility to implement a local chromatic correction.

The unequal β^* also helps for the beam separation. Considering a beam crossing in the horizontal plane, the number of σ_x by which the two beams are separated is given by Δin=

$\theta_c/(\epsilon/\beta_x^*)^{1/2}$. For a given θ_c this inner normalized separation gets smaller as β_x^* decreases. By keeping the same crossing angle and the same product $\sigma_x^* \sigma_y^*$ (beam area), increasing β_x^* and reducing β_y^* achieves the same luminosity, while Δin is enlarged. Conversely, if Δin and the beam area are held constant while the ratio σ_x^*/σ_y^* is increased, the luminosity grows together with the beam size in the crossing plane. Figure 3 shows the luminosity for flat and for round beams. The crossing angle has been varied to keep the beam separation constant at 9.8σ and the beam area ($\sigma_x^* \sigma_y^*$) was held constant. The luminosity rises as the beams become flatter.
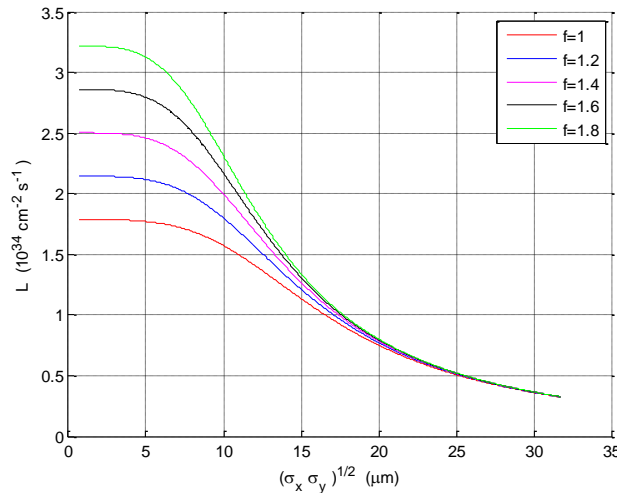

Figure 3: Luminosity for different beam-aspect ratios ($f=\sigma_x/\sigma_y$). The crossing angle is chosen to have an inner normalized separation of 9.8σ in the plane of crossing.

3.2.1. Flat beams for the present LHC

A new optics has been designed for beam tests with moderately flat aspect ratios at the present LHC. The objective is to study "quasi" flat-beam conditions in a Machine Development (MD) session, in order to explore the resulting tune shifts, lifetime, effects of transverse offsets, and especially sensitivity to long-range beam-beam effects.

Figures 5 and 6 show a new quasi-flat optics developed for the present LHC, obtained after a squeeze process from the round beam optics in Fig 4. Specifically, the starting point of the quasi-flat condition is a present LHC optics with $\beta_{x,y}^*$=1.20 m (Fig 4). From this optics, a squeeze in the non-crossing plane was computed for IP1 till β_x^*=0.60 m. The squeeze maintains β_y^*=1.20 m, while intermediate new optics with β_x^*={1.05 m, 0.90 m, 0.75 m, 0.60 m} were matched so as to provide a smooth transition from β_x^*=1.20 m to 0.60 m. The final optics for IP1 is represented in Fig. 5. For IR5 the role of the two planes is changed, in order to have the squeeze in the non-crossing plane, and here the vertical β_y^* is decreased to 0.60 m (see Fig. 6). Two sets of four new optics have been computed for either IR. The possibility of obtaining a considerably smaller value for $\sigma_x^* \sigma_y^*$ is limited by the triplet FF system. Also, a high ratio $\sigma_x^* \sigma_y^*$ is not achievable with conventional single-aperture quadrupole magnets in the triplet.

The magnets whose strength is modified during this squeeze are Q4 to Q10 together with the trim quadrupoles QTLI.11, QT12 and QT13. The computed squeeze was implemented in the LHC control system and the magnet cycle was executed successfully without beam. Due to lack of time no test with beam was possible in 2012.
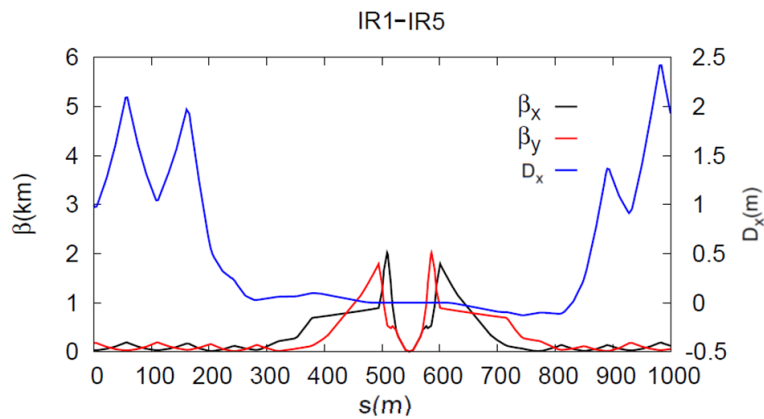
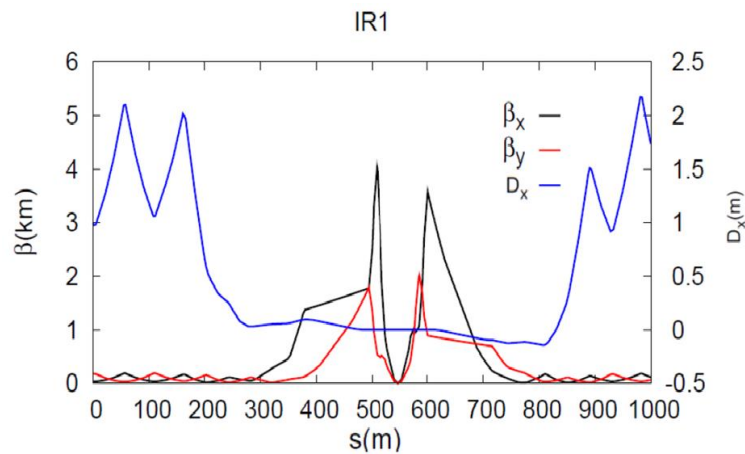*Figure 4: Present LHC IR1 & IR5 Optics with β_x^*=1.2 m, β_y^*=1.2 m.*

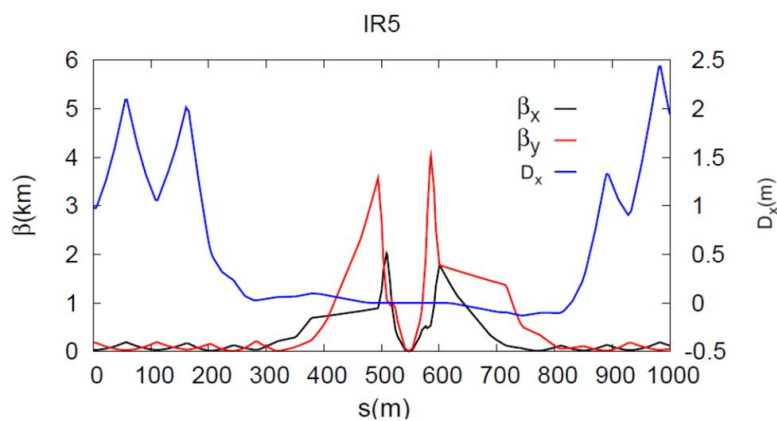*Figure 5: LHC quasi-flat IR1 optics with β_x^*=0.6 m, β_y^*=1.2 m.*

Figure 6: LHC quasi-flat IR5 optics with β_x^*=1.2 m, β_y^*=0.6 m.

Figures 7 and 8 show the current ratios, between Beam 1 and Beam 2, during the squeeze for each pair of implicated two-in-one magnets, at IP1 and IP5, respectively. Due to the actual cabling/powering scheme as well as a possible interplay between the two apertures, this ratio is presently restricted to the interval (0.5, 2). Each magnet is coupled with the equivalent magnet for the other beam, sharing wires, and the current in one magnet should not exceed twice the value of the other. These conditions apply to the main quadrupoles and not to the trim quadrupoles, for which reason the strengths of the latter are now shown in the figures.
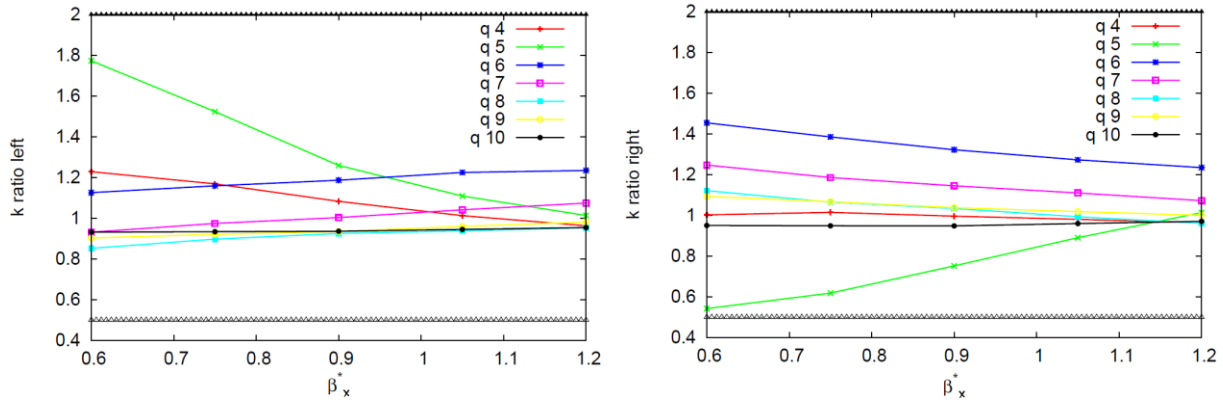
Figure 7: Magnet current ratios for the horizontal squeeze at IP1, left side and right side.
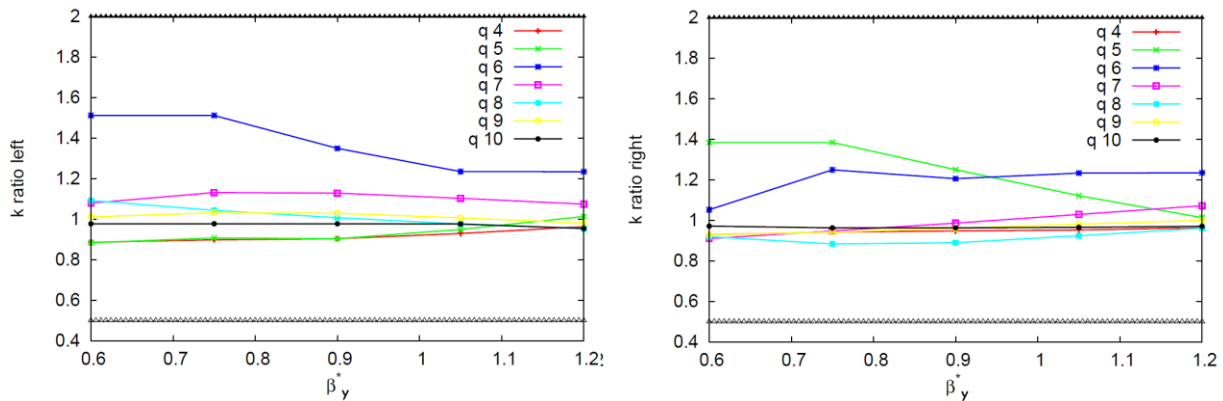

Figure 8: Vertical squeeze (IP5), left side (left) and right side (right).

It was verified that all the powering curves for each individual magnet are monotonic. This monotonicity prevents the magnets from switching between different hysteresis branches.

Another constraint to be considered when designing the new set of optics is the β-beat between the matched optics points. Between two matched optics, the magnet currents are obtained by interpolating from the two end values. However, due to the non-linearity of the system, when all the magnets use interpolated current values, the result is a non-perfectly matched optics and, as a result, there is a small beat of the β-function over the entire ring. Figure 9 shows, for Beam 1 and Beam 2, the maximum of the β beat over all beam-position monitors (BPMs) in IR1 and IR5 for the transition of β* from 1.2 m to 0.6 m. This value is always smaller than 0.6%, and hence negligible.
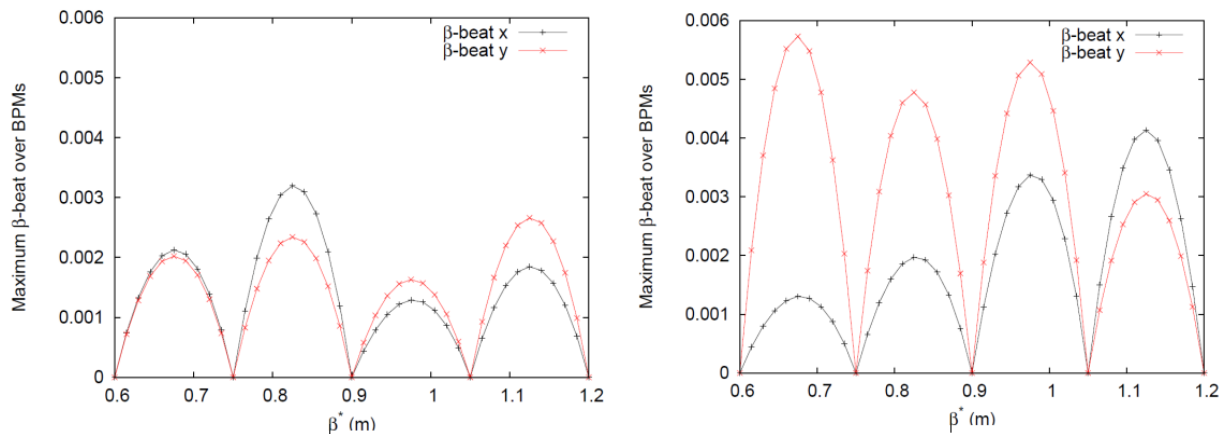
Figure 9: Maximum relative β-beating for the LHC quasi-flat beam optics over all IR BPMs for Beam 1 (left) and Beam 2 (right) as a function of β*.

For the round optics of the present LHC the β–function for each beam are antisymmetric, as illustrated in Fig. 4, that is, the optics for one plane on one side of the IP is identical to the optics of the other beam in the other plane or of the same beam on the other side of the IP in the orthogonal plane. When flat beams are introduced, in Figs. 5 and 6, four different optics emerge, and for each of them, in case of a local chromatic correction, two pairs of sextupoles must be added with a spacing of π in phase advance, rendering very complicated the implementation of a local chromatic correction based on the present LHC optics.

3.3.   LARGE PIWINSKI ANGLE

Collisions with a large Piwinski angle (Φ>1) are considered for future LHC upgrades. They also naturally occur in scenarios for 7-TeV operation with 50-ns bunch spacing after the Long Shutdown 1 (2013/14). The Piwinski angle is increased by reducing the beam size in the plane of crossing. This is the case for future LHC upgrades where a luminosity increase is targeted through a significant reduction in the β-function [10]. The large Piwinski angle can also be enhanced by a corresponding increase in the crossing angle, such as for the crab-waist collision scheme. Though an increase in the Piwinski angle reduces the geometric luminosity as $L \sim (1+\phi^2)^{1/2}$, it also has several advantages: Firstly, it mitigates the hourglass effect thanks to the reduction in the length of the bunch overlap area, supporting a significant reduction of the β*. Secondly, it decreases the beam-beam tune shift by about the same reduction factor as for the luminosity, so that operation at the same tune shift becomes possible while storing much brighter beams [1]. On the other hand with a transverse offset the longitudinal collision point (CP), given by the encounter with the axis of the opposite beam, is moved with respect to the ideal IP, thus exciting betatron and synchro-betatron resonances by the coupling of transverse and longitudinal motion. Also, the large Piwinski angle breaks the collision symmetry, which may be essential for operation with a high beam-beam parameter [11,12].

Strong-strong simulations for the LHC MD configuration were performed by K. Ohmi (KEK, Tsukuba. Japan). The simulation results are shown in Fig. 10, where the simulated luminosity and the luminosity decay per turn are plotted as a function of the half crossing angle.
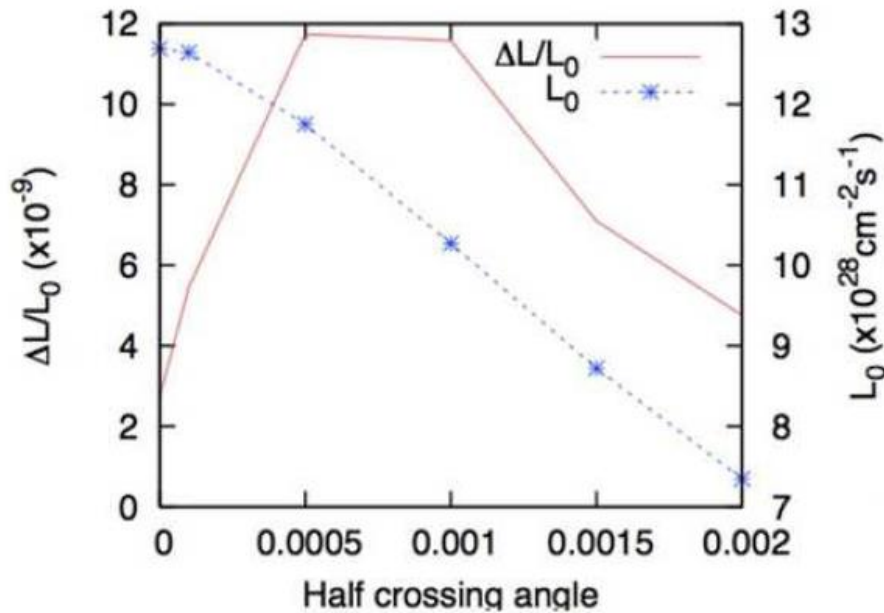
Figure 10: Simulated MD luminosity and luminosity decay per turn as a function of the half crossing angle in IP8 for the LHC at injection, with simultaneous collisions in 3 IPs (1, 5, 8).

There are two competing effects of the Piwinski angle on the luminosity lifetime: (1) the beam losses increase as a consequence of the excitation of nonlinear betatron and synchro-betatron resonances; (2) the beam-beam tune shift gets reduced through a decrease in the geometric reduction factor. As can be seen in the figure, the first effect is dominant for crossing angles smaller than about 0.5 mrad, and it roughly compensates the effect of the second between 0.5−1.0 mrad. Finally, for crossing angles bigger than 1.0 mrad the second factor dominates and the luminosity lifetime increases significantly, while the value of the luminosity and the beam-beam tune shift decrease.

The actual MD was performed on 19 June 2012 [Abe05] to study the effect of the LPA on LHC luminosity and to benchmark the simulation. Two high brightness bunches per beam were collided at 450 GeV (injection energy) with varying IP8 spectrometer strength so as to change the Piwinski angle ϕ at IP8 in the range 0.2-1.2, achieving the highest value of ϕ ever reached in a hadron collider. The first of the two bunches, called A, experienced a single collision in IP8 only; while bunch B suffered collisions in IP1, IP5 and IP8. The experiment was not fully conclusive due to unrelated technical problems and missing luminosity data from two LHC experiments. Table 1 shows some of the results obtained, namely the bunch lifetimes at different spectrometer settings (crossing angles). The control of the experimental conditions was insufficient, and the results were not fully conclusive. For details see [Abe05].

Table 1: Bunch lifetimes in hours for different strengths of the IP8 spectrometer; spectrometer strength of 100% corresponds to a half crossing angle of about 2 mrad or to ϕ~1.2.

spectr. strength	beam 1, b. A	beam 1, b. B	beam 2, b. A	beam 2, b. B
100%	4.8	1.44	7.6	1.25
50 % (30 s. interval)	3.0	2.0	5.8	1.6
50 % (ext. interval)	2.7	1.7	5.2	1.44
minimum	3.0	3.5	5.0	1.9

In any case, the strong-strong beam-beam simulations suggest that LPA operation may overcome one of the main limitations for hadron collider luminosity, namely the upper bound on beam brightness.

3.4. CRAB-WAIST COLLISIONS

The resonances introduced by the LPA can be removed by means of a novel technique first introduced in DAΦNE [13], which consists in restoring, for particles with different *x*-coordinate at the IP, the ideal longitudinal IP. This is done by the installation of two sextupoles with opposite sign on each side of the IP and for the two beams, at appropriate, but unusual betatron phase advance in the two planes. These sextupoles can increase luminosity by further mitigating the hourglass effect, but their main purpose is to suppress resonances, thereby allowing for higher tune shifts and LPA operation. A test was performed in DAΦNE that consisted in switching off and on the sextupoles for the two beams, and to analyse the resulting effect on the beam sizes (Fig 10). Switching off the CR-W sextupoles in both beams produced a significant increase in the horizontal beam size. Figure 11 shows pertinent readings from the DAΦNE control system, illustrating that the luminosity shrinks when the CR-W sextupoles are off, while the background increases.
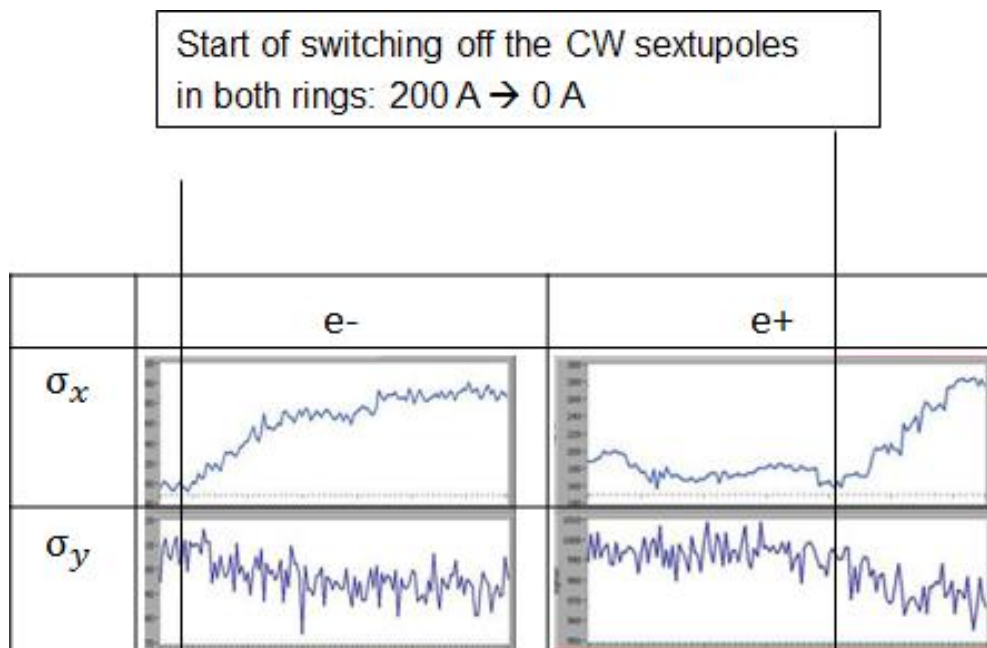

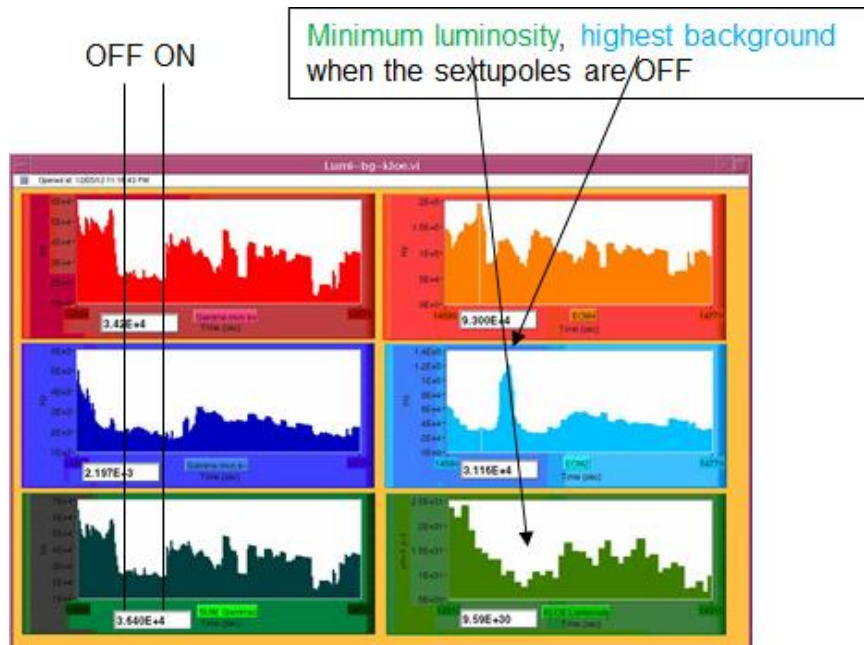*Figure 10: DAΦNE beam sizes for e- and e+ during the crab-waist experiment.*

Figure 11: DAΦNE luminosity readings during the crab-waist experiment.

4. APPLICATION OF FREQUENCY MAP ANALYSIS TO BEAM-BEAM EFFECTS STUDY IN CRAB WAIST COLLISION SCHEME

A study over the effectiveness of crab-waist collision scheme applied to LHC was performed [Shat01] (The pertinent journal article was selected as one of the seven PRST-AB highlight papers from 2011). In this work, frequency map analysis (FMA) [14] – a method that is widely used for exploring the dynamics of Hamiltonian systems – , has been applied to study beam-beam effects in the crab-waist collision scheme. As expected, under the right conditions, the crab-waist focusing of colliding beams can result in a significant suppression of betatron coupling resonances induced by the beam-beam interaction. Application of FMA provides visible information about all working resonances, their widths, and locations in the planes of betatron tunes and betatron amplitudes, so that the process of resonance suppression due to the beam crabbing is clearly revealed. Figure 12 shows an example footprint with CR-W sextupoles off and on. As we can see switching on the crab-waist sextupoles has two beneficial consequences: a smaller footprint area and a considerable reduction of the beam-beam resonance strength.
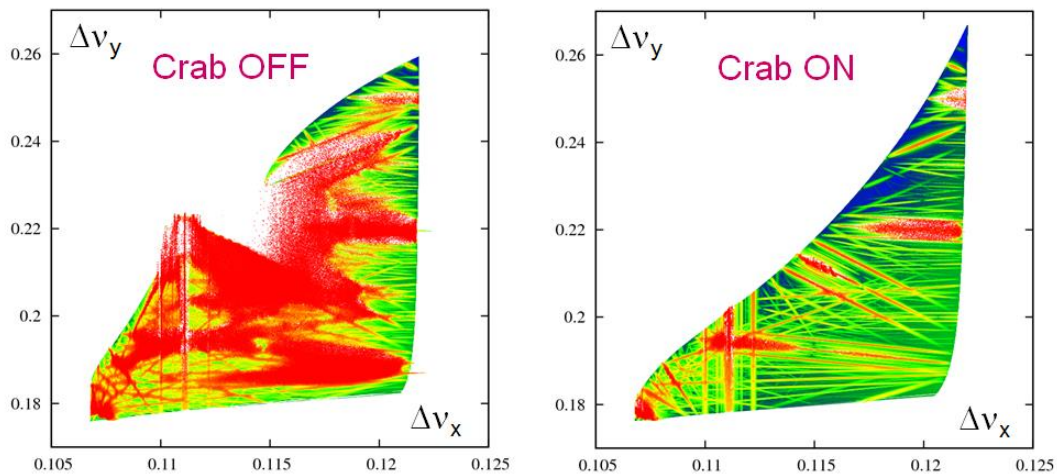
Figure 12: Resonance plot of the tunes, showing the resonances [Shat01].

4.1.   CRAB-WAIST COLLISIONS FOR LHC

The aforementioned FMA technique has been used to explore the beam dynamics in the LHC. Figures 13 and 14 show an example for θ_c = 1.5 mrad and σ_x^*/σ_y^*=10. Here tune-diffusion values are plotted in two different planes: in the plane of the betatron tunes, i.e. the so-called tune foot prints (left pictures) and in the plane of normalized betatron amplitudes (right pictures). Figure 13 refers to a situation without crab-waist sextupoles, while Fig. 14 shows a case in which the sextupoles are switched on at 50% of their nominal strength. The blue color indicates stable motion and the red color signifies stochasticity.
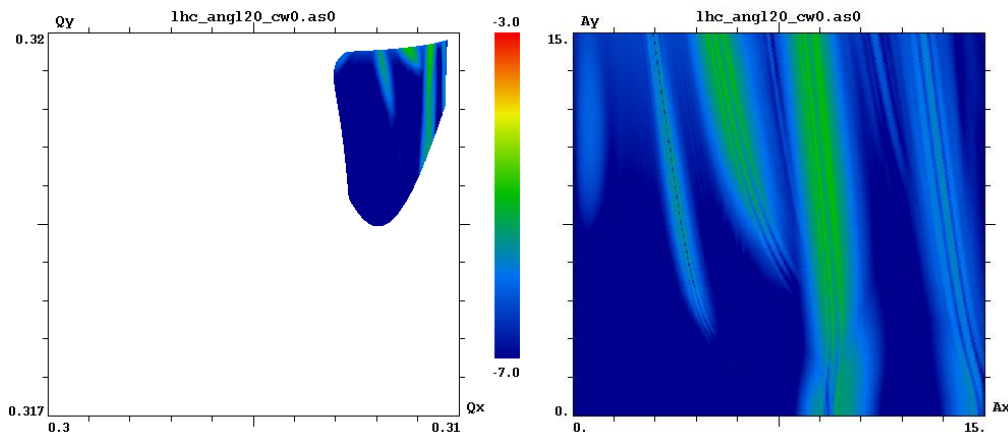

Figure 13: LHC resonance plot without crab-waists [Shat01]. Betatron tunes (left) and normalized betatron amplitudes (right).
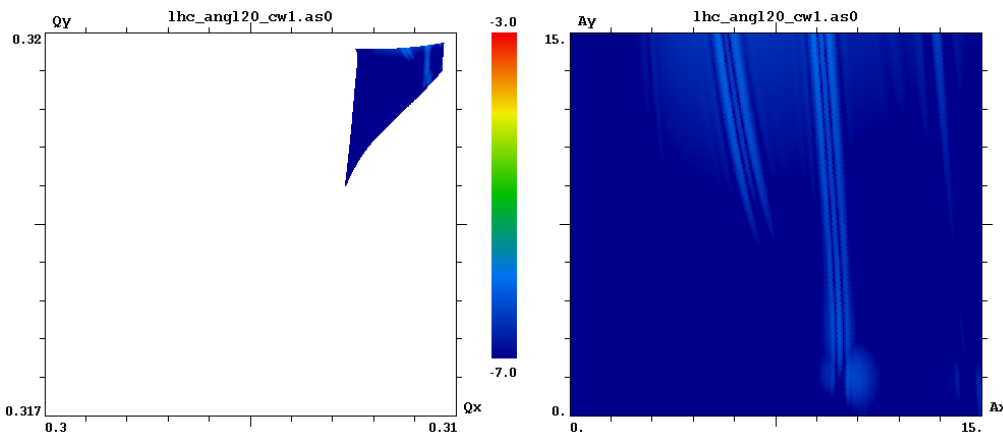
Figure 14: LHC resonance plot with crab-waists sextupoles at half strength [Shat01]. Betatron tunes (left) and normalized betatron amplitudes (right).

As in the case for DAΦNE, the widths of the resonances in the footprint are reduced. Therefore, by exploiting the crab sextupoles one can expect a better beam-beam performance in terms of luminosity and beam lifetime, as well as the potential of higher beam-beam tune shifts.

The most important conclusion of the detailed FMA study for the LHC [Shat01] is that the crab-waist scheme is not effective for round beams, and that IP aspect ratio of at least $\sigma_x^*/\sigma_y^* > 10$ is required in order for a CR-W scheme to work at full strength.

We have, therefore, aimed at designing an LHC optics with an aspect ratio of 10 or the equivalent β* ratio of 100.

5. AN LHC IR WITH LOCAL CHROMATIC CORRECTION, FLAT BEAMS AND CRAB-WAIST COLLISIONS

5.1. MOTIVATION

The IR presented here makes use of all the ideas discussed previously. It is likely that the local chromatic correction and crab-waist sextupoles can be made to conspire, removing one of the main performance limitations of the LHC. However, there are several facts that render difficult the implementation of crab-waist collisions in **LHC**, compared with **DAΦNE.**

- **Same charge of the particles:** the focusing elements must have opposite sign for the two beams, including the last quadrupole where the two beams should be in the same aperture.

- **Large L* (23 m, 20.4 cm).** This generates high values of the β-functions in the final-focus, generating a large chromaticity.

- **Large Energy (7 TeV, 0.51 GeV).** In order to have elements with high quadrupolar strength, the gradients and the magnetic fields must also be very high. (Advanced) superconducting technology is required.

- **Same emittance in the two planes ($\varepsilon_x/\varepsilon_y$=1, εx/εy=200).** Because of the absence of radiation damping, the beam distribution does not attain the equilibrium and the near-unity emittance ratio between the two planes is preserved throughout the physics store. A high beam size ratio translates into a very high β ratio.

In response to these challenges, a new IR has been envisioned with the following components:

- **Large Piwinski angle:** To allow higher brightness beams. By means of a large θ_c the beams are sufficiently separated to pass through the novel DHQ magnet. The LPA also allows a significant β_y^* decrease by reducing the length of the collision region.

- **Flat beams:** To separate the two transverse β functions allowing for a local chromatic correction. They also provide a better normalized separation.

- **Symmetric optics.** The small values of β_y^* considered for extremely flat beam collisions (a few cm) cannot be reached for a standard quadrupole magnet with the same field gradient acting on both beams in a common aperture, as for the nominal LHC, since in that case the vertical beta function of one of the two beams (and/or on one side of the IP) would become so large as to render the chromatic correction impossible using available sextupole strengths. A symmetric optics for the LHC interaction region had already been studied in the distant past [19]. This earlier optics was symmetric for each beam as it featured the same quadrupole-strength distribution on the two sides of the IP. However, it still was anti-symmetric with regard to an interchange of the two beams, since the beams shared the same magnetic fields and, therefore, experienced quadrupolar focusing of opposite sign.

- **Chromatic correction in the IR:** To allow for low values of β_y^* and to increase the dynamic aperture.

- **Crab-waist collisions.** To suppress the X-Y resonances excited by the beam-beam interaction, allowing for higher tune shifts and increasing the dynamic aperture.

5.2. DESIGN CONSTRAINTS

A completely new IR has been designed. According to the simulations cited earlier [Shat01], the optimum beam size ratio for crab-waist collisions is σ_x^*/σ_y^* >10.   Assuming equal emittances in the two planes, this implies β_x/β_y =100. In our first optics, the product $\beta_x\beta_y$ was chosen to be equal to that of nominal ATS optics with crab-cavities, that is $\beta_x^*\beta_y^*$=(15 cm)^2. The optical functions at IP are then β_x^*=1.5 m and $\beta_{y.}^*$=1.5 cm. The final triplet with common aperture for the two beams should be replaced by a set of four lenses, (the latter) 3 of which normal quadrupoles with separate aperture, in order to provide the optical symmetry between the two beams. That means that the gradients must have opposite sign for the two beams, unlike for the present arc quadrupoles, where at present the gradients have the same sign. In order for the last quadrupole to host the two beams in different apertures, the crossing angle should be 194 mm/23 m = 8.4 mrad, an excessive value that would lead to a very low geometric reduction factor. Inspired by the LHeC "half-quadrupole" design [Abe03], a double half quadrupole has been conceived to build a symmetric optics. Figure 15 shows a sketch comparing the present LHC IR scheme, and the one proposed.
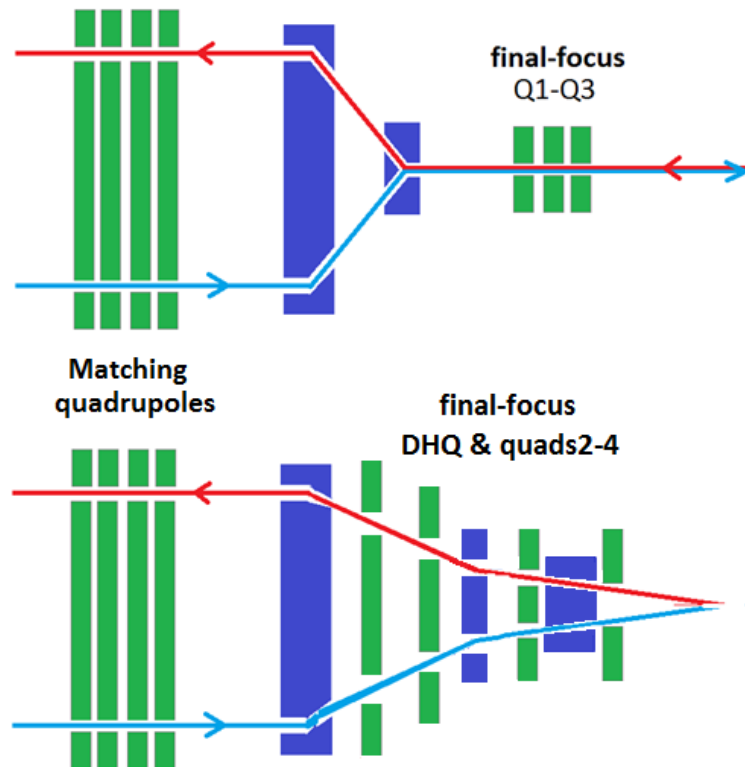
Figure 15: Schematic comparing the LHC crossing scheme and the proposed flat-beam scheme. The reference orbits for both beams are indicated. Bending magnets are shown in blue and quadrupoles in green.

The present IR of LHC features two separator dipole magnets. This brings the beams to a common aperture in the final focus, consisting of a triplet. These separator magnets divide between the magnets where the two beam share a common aperture and those with separate apertures. Orbit-corrector bumps are used to modify the closed orbit so that the beams cross each other at the IP at a certain angle in one or the other plane. In the proposed IR, however, the DHQ is the only focusing element where the beams occupy the same aperture, and the separator bending magnets are interleaved with the quadrupoles. The final DHQ must provide a quadrupolar gradient of opposite sign for the two beams.

5.3. THE DOUBLE HALF QUADRUPOLE DESIGN

The design of this element has been developed in collaboration with S. Russenschuck (CERN) using the code ROXIE [15]. Choosing a rectangular aperture (which would not be possible with pure sextupole geometry) allows accommodating two side-by side beam pipes of elliptical dimensions. For small gradients and apertures half-quadrupoles can be constructed with a mirror-plate made from soft-magnetic steel. Such a type of magnet was installed in the IRs of the HERA *ep* collider and at the KEK B-factory [16]. The required high gradient requires the use of superconductor technology for the coils. However, the fields implied would result in a complete saturation of the mirror-plate. Therefore, the solution proposed is a combined function magnet consisting of eight racetrack coils that produce a combined dipole and sextupole field in a common aperture, without any mirror plate; see Fig. 16. We assume LHC inner and outer layer Nb-Ti cable, operated at 80% on the load-line. The peak field in the coil is 8.14 T for an aperture square of 160 mm, and the gradient at the centre of the beam (45 mm from the origin) is 116 T/m, with an additional dipole field component of 5.5 T. We

note that also some general analytical solutions are available for producing field configurations with two beams of minimum separation by the optimized placement of individual SC wires [17]. The simple (non-optimum) racetrack shape chosen for the SC coils of Fig. 16 will facilitate the use of Nb₃Sn technology if required. The field shape of the DHQ is shown in Fig.17. Since the design orbits of the two beams are separated by 90 mm, the feed-down from the strong sextupole produces the desired strong quadrupole component, of opposite sign for the two beams. [Abe05].
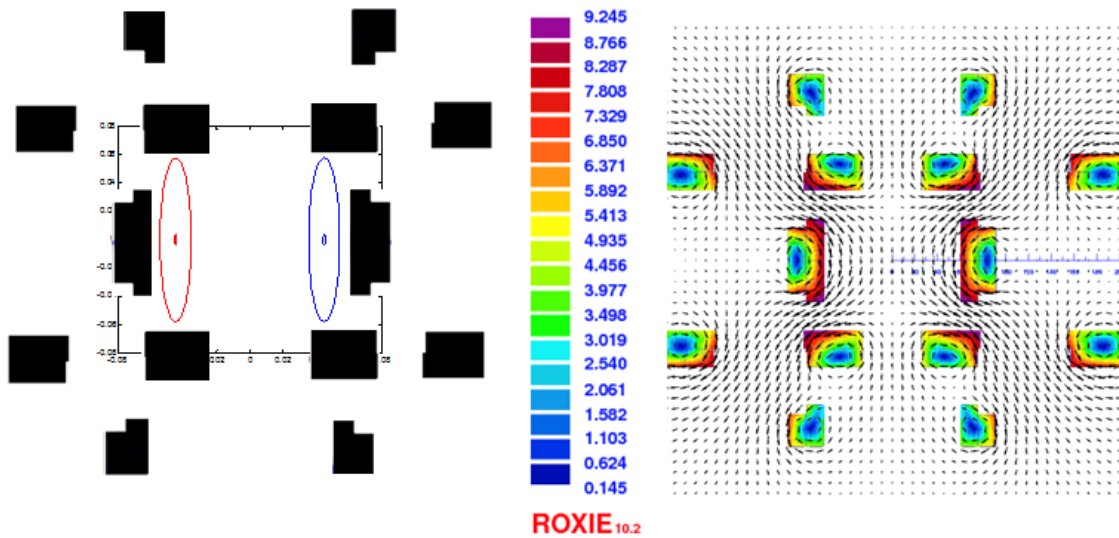

Figure 16: Cross section of the double half quadrupole DHQ. The coils are wound from simple racetracks in order to facility the production in case Nb₃Sn superconductor technology would be required.
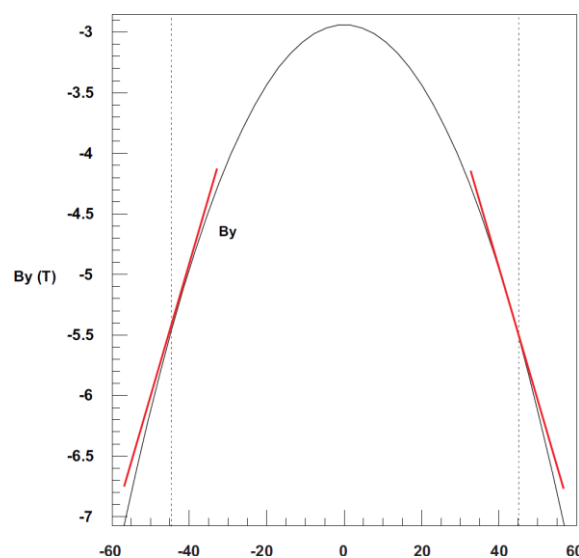

Figure 17: Magnetic field distribution for the DHQ computed by ROXIE.

The complete design of the IR relies on this element. Its maximum achievable gradient determines the length of the DHQ. Figure 18 presents the absolute value of multipolar components,

$$ B_{n+1} \propto \frac{r_0^{\,n}}{n!} \frac{\partial^n B_y}{\partial x^n} \ , $$

normalized to B2 (the quadrupole field a the design orbit) in units of 10^{-4}, and for a reference radius r_0=17 mm. Only for multipole components of order higher than 7 is the component below 1. B3 is very high, and it could help to correct the chromatic aberrations by setting the dispersion to an appropriate value. The geometric aberrations can be cancelled by placing a sextupole at an appropriate phase advance.
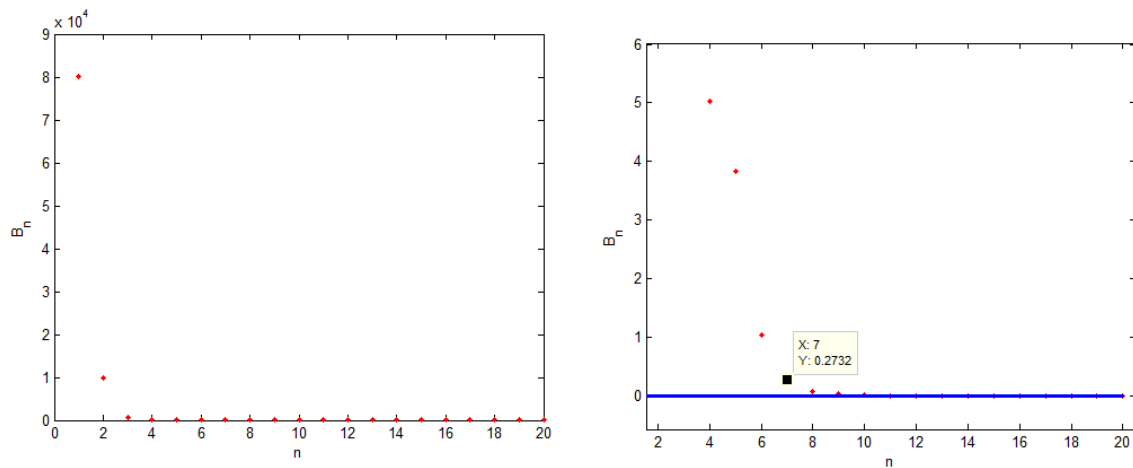

Figure 18: Multipolar components of the DHQ (left) and detail (right). for a reference radius r_0=17 mm and normalized to the quadrupole field.

5.4. PARAMETER ANALYSIS OF THE DHQ

The beams enter the DHQ at a certain angle. For a long element (in the proposed design it has length of 14 m), the separation of the beams would intolerably increase. The effect of the dipolar field term will also further increase the beam separation. Large change in the separation may result in the beams no longer fitting inside the available window or reduce the effective gradient. For these reasons the DHQ element should ideally be built in segments, as illustrated in Fig. 19.
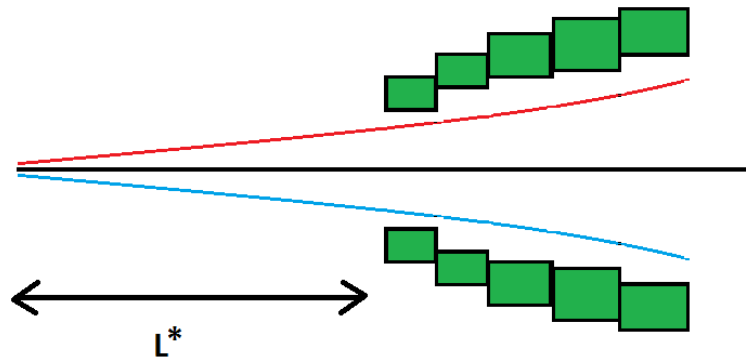
Figure 19: Schematic of the final double half quadrupole DHQ including segmentation.

The properties of the quadrupole and sextupole fields are known. Considering a circular aperture with radius r, and a quadrupole gradient g the magnetic field at the aperture $B = gr$ grows in proportion to the radius. For a sextupole with sextupole strength k_s, the field at the aperture is $B = \frac{1}{2}\, g_s r^2$, i.e. it grows a square of the radius. From these scaling laws, we can deduce how the gradient changes by varying the aperture and keeping a constant peak field at the aperture. However, when doing so, the higher-order multipolar components also vary, and the geometry of the various DHQ coils may need to be modified to keep these multipoles under control. Therefore, ultimately we need to re-optimize the DHQs for different apertures. In a related study the beam offset Δx was shifted together with the horizontal dimension of the aperture of the DHQ (by $2\Delta x$), keeping the vertical aperture constant (Fig. 20).
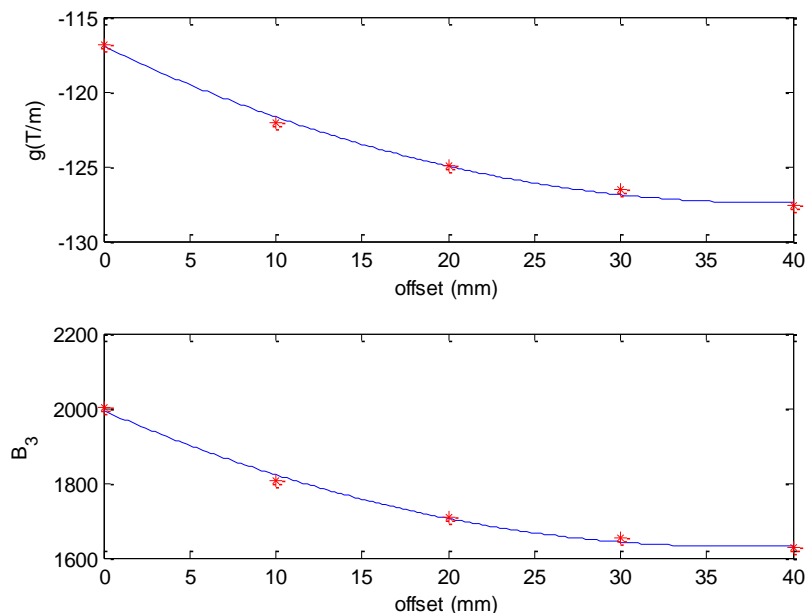

Figure 20: Variation of DHQ gradient and sextupole B_3 (normalized to the nominal quadrupole field in units of 10^{-4} as a function of horizontal offset from the nominal reference point.

5.5. SEXTUPOLAR COMPONENT OF THE DHQ

Figure 21 shows the approximate field distribution in the DHQ on both sides of the IP and for both beams, in order to deduce the signs of the multipolar components for the different cases. The signs of the dipole and sextupole terms are inverted for Beam 2 since the longitudinal component of the velocity is opposite to that of Beam 1.
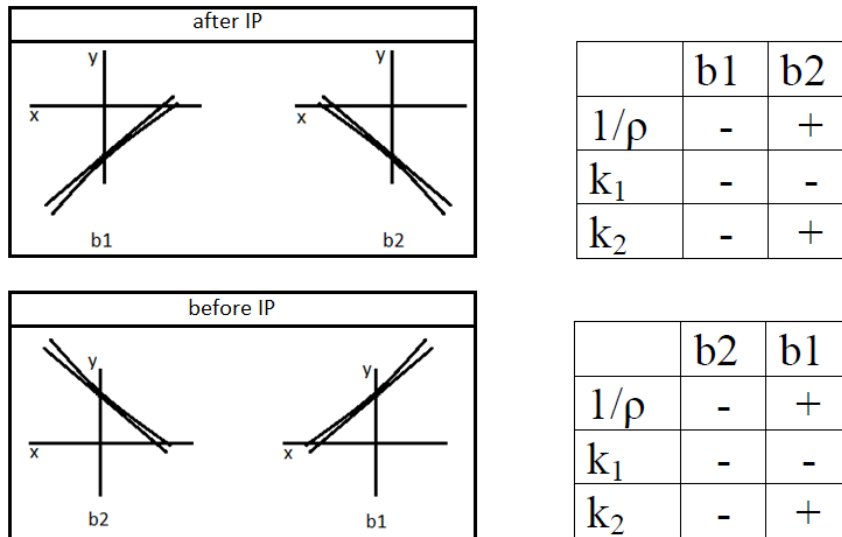

	b1	b2
$1/\rho$	-	+
k_1	-	-
k_2	-	+

	b2	b1
$1/\rho$	-	+
k_1	-	-
k_2	-	+

Figure 21: Approximate field distribution of the DHQ for both beams on either side of the IP.

In all cases the dipolar component enhances the beam separation away from the IP. The significant sextupolar component can be exploited as an intrinsic chromatic sextupole. To do so, the signs of the dispersion in the DHQ must be positive for Beam 1 after the IP and for Beam 2 before the IP, and negative for the other two cases. Then in all four cases, this sextupolar component combined with the dispersion in the DHQ results in a chromatic correction with a positive sign. Unlike the β-functions, the dispersion will be naturally antisymmetric without additional dipole magnets between the two DHQ on either side of the IP. The symmetry is broken through the non-zero derivate of the dispersion at the IP, and further enhanced by the antisymmetry of the separation magnets. A sketch in Fig. 22 shows the signs of dispersion, quadrupolar and sextupolar components for all four cases.
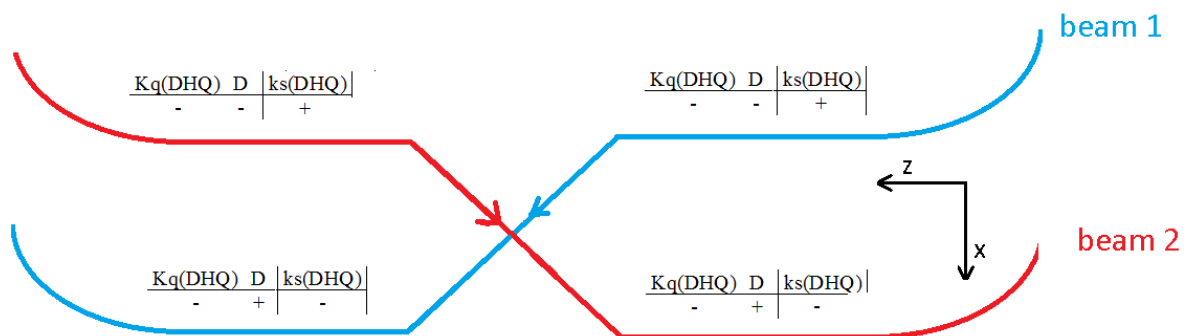

Figure 22: Schematic reference orbits of the two beams, together with signs of DHQ quadrupolar strength, of the dispersion, and of the DHQ sextupolar component.

5.6. OPTICS

5.6.1. Interaction region - 1st design: Local chromatic correction in the vertical plane

A first exploratory design for the new IR was proposed in [Abe06, Abe07]. The IR was matched to the arcs on both sides of the IP and it allowed the installation of one pair of sextupoles at the peaks of the vertical β-function (Fig. 23) for a local correction of the vertical chromaticity only.
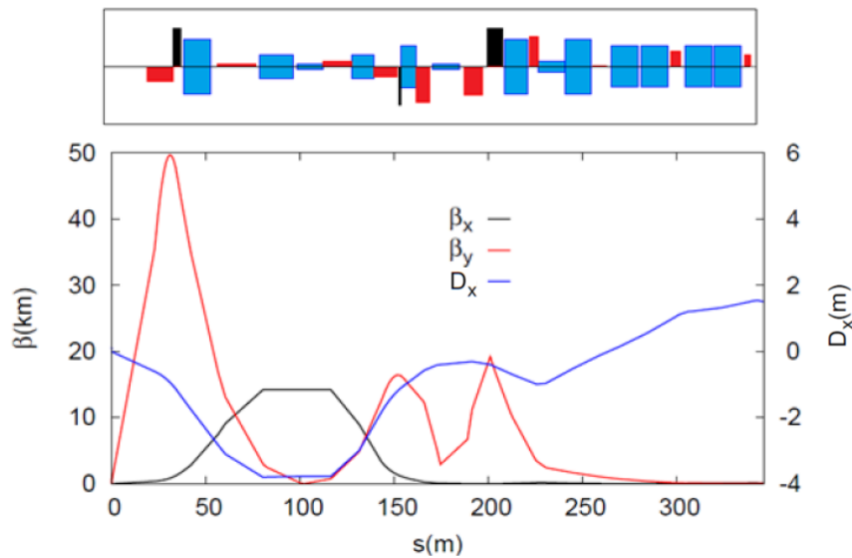

Figure 23: LHC flat-beam IR optics (right side of the IP). Bending magnets are shown in blue, quadrupoles in red and sextupoles in black.

Additional bending magnets were installed to close the orbit (Fig. 24). This design required an optimization of the dispersion function at the two sextupoles, in order to correct the vertical chromaticity. There was no possibility to locally correct the horizontal chromaticity with this design, whose main purpose was to test the possibility of matching from the LHC arcs to the IR with

- extreme optical values at the LHC IP, namely β_x^*/β_y^*=100, β_y^*=1.5 cm,
- a place to install a crab-waist sextupole.

Concerning the last point, a place was found with the following optics at the entrance and at the exit of the crab-waist sextupole, with a length of 8 m (Table 2).

Table 2: Optical values of the crab-waist sextupole entrance and exit

	Sextupole entrance	Sextupole exit
$\Delta\mu_x$ from IP (2π rad)	0.49	0.521.25
$\Delta\mu_y$ from IP (2π rad)	1.25	1.25
β_x (m)	23.2	58.6
β_y(km)	16.6	10.6

With these values, the crab-waist sextupole would need a normalized strength of 0.0313 m^{-3}.
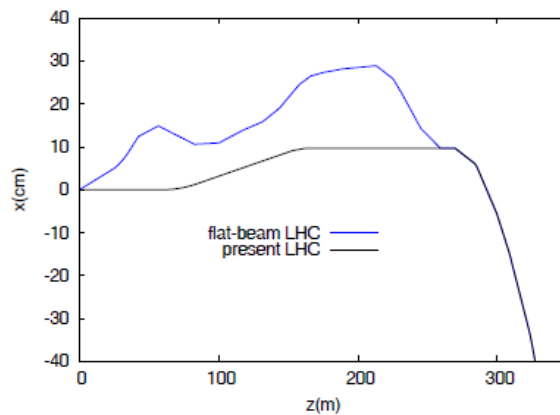
Figure 24: Reference orbit footprint of the first design compared with the actual LHC.

5.6.2. Interaction region – 2nd design: Local chromatic correction in both planes

A second design was made, including two peaks of the horizontal β-function, in order to install two additional IR sextupoles to also locally correct the horizontal chromaticity. It is shown in Fig. 25 [Abe08].
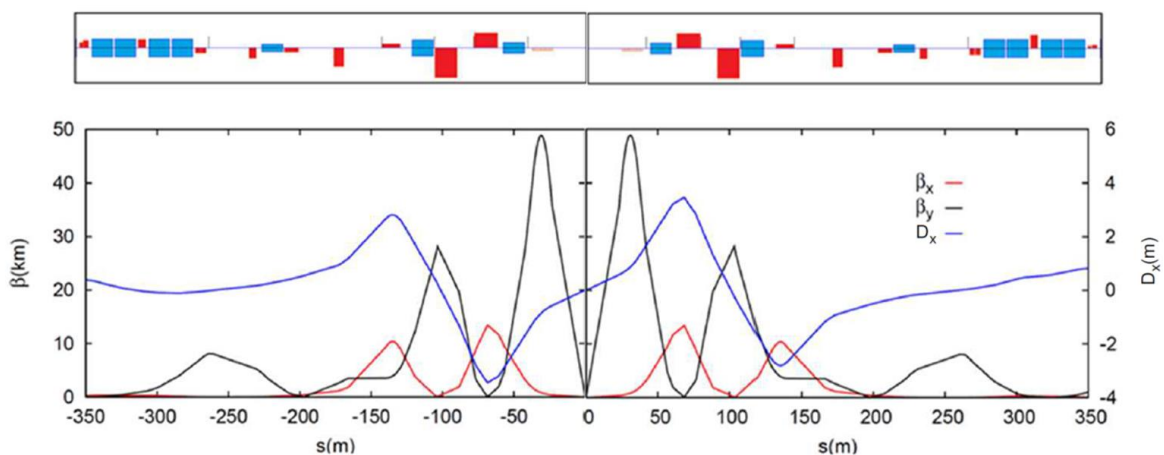

Figure 25: Interaction region for the second design.

The new interaction region is created by replacing the existing triplet with a set of 4 new quadrupole lenses. The DHQ is the final lens. The parameters of the other three quadrupoles are summarized in Table 3. The aperture radius has been chosen so as to fit a 15σ ellipse with a normalized r.m.s. emittance of 2.2 μm.

Table 3: Final-focus quadrupoles for the second design. Gradient, aperture radius and length.

	g (T/m)	a (mm)	L(m)
quad2	93.4	30	16
quad3	-98.9	44	15
quad4	105.8	26	4

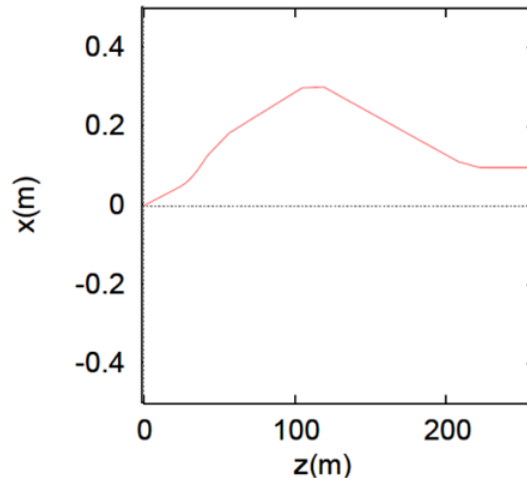The reference orbit for this design is shown in Fig 26.

Figure 26: Reference orbit footprint of the second design compared with the actual LHC.

5.6.3. Sextupoles and local chromatic correction

A total of 5 sextupoles per side and per IP are added, installed at the respective peaks of the β-function. Table 3 shows the phase advances from the IP of all these sextupoles. Sextupole sext1 corrects the vertical chromaticity while sext2 corrects the horizontal one. Sext3 and sext4 are placed where the dispersion is zero. They compensate the geometric aberrations induced by sext3 and sext4, respectively, without inducing any chromatic effect. The last sextupole, sext5 is the crab-waist sextupole. Its phase advances comply with the requirements (3.1). The absolute value of the integrated nominal strength, according to these optics parameters, is, $k_{sl} = 0.61\text{m}^{-2}$. As for the other sextupoles, they are grouped in pairs. For each pair one sextupole carries out the chromatic correction and the other corrects the geometric aberration created by the former.

Table 4: Sextupoles for the second design: phase advances, beta-functions and dispersion

	$\Delta\mu_x$(rad)	$\Delta\mu_y$(rad)	β_x (m)	β_y(m)
Sext1	$\pi/2$	$\pi/2$	834	48923
Sext2	$\pi/2$	$\pi/2$	11654	1943
Sext3	$3\pi/2$	$3\pi/2$	125	27580
Sext4	$3\pi/2$	$3\pi/2$	9251	3546
Sext5	π	$5\pi/2$	18	7872

5.6.4. Crab-waist sextupoles

The cr-w sextupoles, if located where the dispersion is non-zero, contribute to the chromaticity. A non-zero dispersion would decouple the activation of the cr-w collisions from the chromatic correction. If this is not possible, the dispersion at the cr-w sextupoles must have the signs indicated in Table 5, in order for the sextupoles not to fight against the chromatic ones. By adjusting one of them to the proper value, the dispersion for the second one, on the other side of the IP, will automatically have the necessary sign.

Table 5: Required signs of the dispersion at the cr-w sextupoles for these sextupoles to assist in correcting the chromaticity.

	Before IP	After IP
Beam 1	+	-
Beam 2	-	+

6. AN ALTERNATIVE OPTICS WITH LOCAL CHROMATIC CORRECTION IN THE VERTICAL PLANE

An alternative design was presented in [Abe09]. The extreme value for the optics at the IP considered in Section 5 led to an excessive value for the vertical β-function, (~50 km), resulting in a large chromaticity. It has proven difficult to correct the chromaticity locally, together with a local horizontal correction, without creating other noticeable aberrations. In particular, the dynamic aperture proved too small. In order to reduce the chromaticity, the $\beta^{*}_{x,y}$ values have been increased (β_x^{*}=3.5 m, β_y^{*}=3.5 cm) which allows for a simplification of the chromatic correction, so that only the vertical chromaticity now needs to be corrected locally, while the horizontal chromaticity has become sufficiently small to be corrected using the arc sextupoles. The crossing angle has been decreased from 4 mrad to 2.6 mrad.
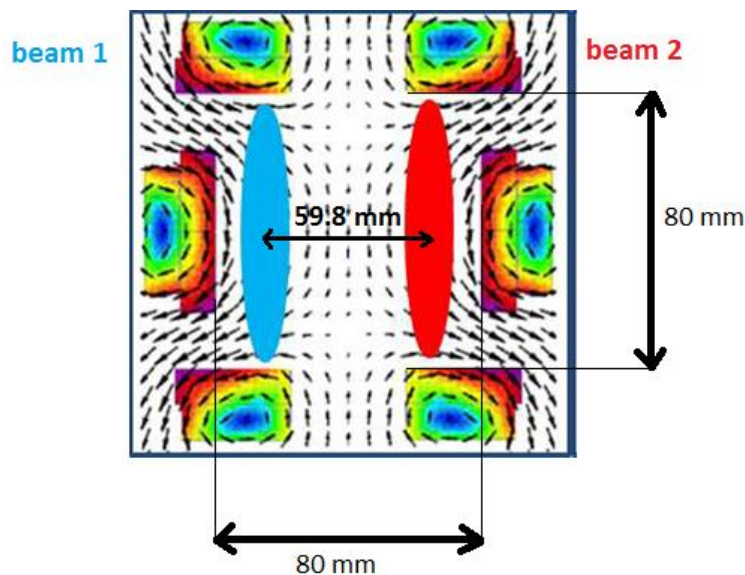

Figure 27: Maximum beam sizes in the DHQ represented as 15-σ ellipses fitting into a square window of 80x80 mm for the alternative optics.

6.1. OPTICS

Thanks to the reduction of the β-functions inside the DHQ and the simultaneous reduction in the crossing angle, the square aperture of the DHQ can be reduced from 120 mm to 80 mm. We also assume that the magnetic quadrupole and sextupolar field components both drop by 20%, at the location of the beam, as a consequence of the combined effect of the smaller aperture, modified magnet geometry, and the reduced crossing angle. The corresponding normalized gradients are K_Q = 0.004 m^{-2} and Ks = 0.047 m^{-3}. Considering a normalized rms emittance of ε_N = 2.2 μm, the maximum beam size in the DHQ is represented as a 15-σ ellipse

with dimensions a_x=6.7 mm, a_y=38.5 mm (Fig. 27). In this scheme, the inner normalized separation is ~$280\sigma_x$, i.e. 30 times higher than for the present LHC.
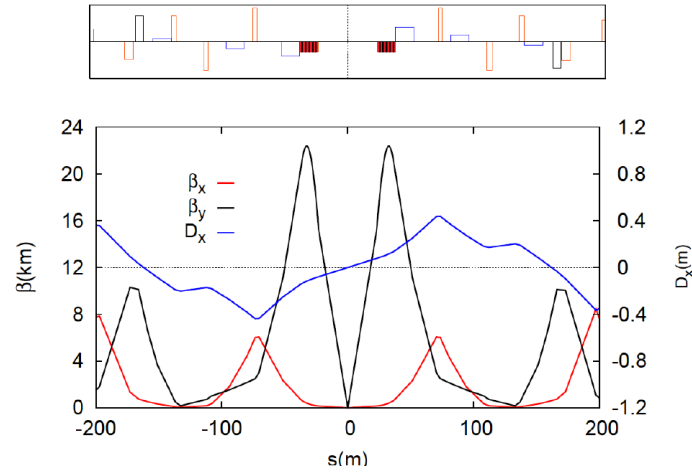

Figure 28: LHC flat-beam IR optics for Beam 1. Bending magnets are shown in blue, quadrupoles in red and sextupoles in black.

The optics for Beam 1 is shown in Fig. 28. It is a symmetric optics. For Beam 2, the β-functions are identical but the bending magnets have opposite sign, and so has the dispersion. The maximum of the β-functions are $\beta_x \sim 680$ km, $\beta_y \sim 22$ km. Quadrupole parameters are summarized in Table 6.

Table 6: Parameters. Normalized gradient, length and aperture

	K [T/m]	Length [m]	a [mm]
Quadrupole 1	322	3.0	21
Quadrupole 2	275	4.0	9
Quadrupole 3	247	4.0	7

6.2. CHROMATIC CORRECTION IN THE VERTICAL PLANE

The vertical chromaticity, Q'_y, is compensated directly in the DHQ, making use of the large sextupole component and nonzero dispersion in this magnet. Specifically, the slope of the dispersion, D'_x, is non-zero at the IP. Its value has been matched so that the sextupolar component in the DHQ corrects the vertical IR chromaticity Q'_y. One more sextupole at each side of the IP, placed in a zero dispersion region and with a phase advance of $\Delta\mu_x = \pi$, $\Delta\mu_y = \pi$ from the centre of the DHQ compensates most of the geometric aberrations. AS an illustration, Table 7 lists the total chromaticity for the LHC with the new IR introduced at IP1 and the present nominal IR (with $\beta^*_x = \beta^*_y = 0.55$ m) remaining in IP5. The total chromaticities for both planes are shown for the quoted strengths of the focusing (k_{sf}) and defocusing arc sextupoles (k_{sd}).

Table 7: LHC chromaticity with alternative flat-beam IR at IP1

$k_{sf}[m^{-3}]$	0	0.1035	0.1727
$k_{sd}[m^{-3}]$	0	-0.1709	-0.1833
Q'$_x$	-246	-107	2
Q'$_y$	-122	11	2

With all the arc sextupoles set to zero, the horizontal chromaticity Q'_x is much higher than the vertical Q'_y, because it is not locally compensated. The second column represents the case where the arc sextupoles are excited at the strength needed to correct the chromaticity in the present LHC to $Q'_x = 2$, $Q'_y = 2$. There is still a large residual Q'$_x$. This can be compensated by setting the sextupole strengths as shown in the third column. If the new flat-beam IR is to be introduced in IP5 as well, the arc sextupoles alone cannot be excited strongly enough to correct the full horizontal chromaticity. Another correction scheme should then be used. Possible solutions include the Achromatic Telescope Squeeze [4], which creates a beta beating in the arc, thereby enhancing the effective sextupole strength, usage of the sextupole spool pieces in the dipole magnets, or a dedicated local correction for the horizontal plane in the IR region.

6.3. SEPARATION SCHEME

Three bending magnets are installed in place of the present LHC dipole separator magnets D1 and D2. Apart from separating the beams and providing the crossing angle at the IP, these bending magnets also bring the dispersion down to zero at the compensator sextupole. Their dipole length has been chosen equal to the one of the LHC bending magnets (14.3 m), and a technology similar to that of D2 can be used. Figure 29 compares the geometry of the new separation scheme with the existing one.
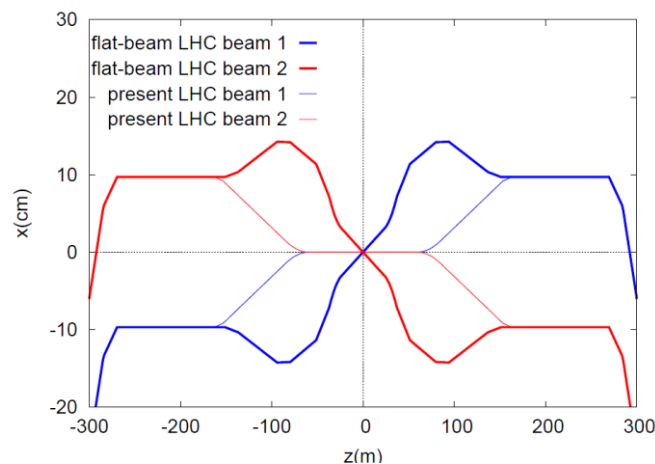

Figure 29: LHC reference orbits in the straight section for the new flat-beam optics, compared with the present LHC.

6.4. LUMINOSITY

Figure 30 illustrates the peak luminosity and the beam-beam parameter as a function of bunch intensity for one interaction region with the new flat-beam optics. In case the flat-beam IR is substituted in both IP1 and IP5, as the crossing takes place in the horizontal plane in either IP, the values of the total beam-beam tune shifts ξ_x and ξ_y are doubled, still remaining below

0.01. For the present LHC, bunch populations above 3×10^{11} would not be possible at the same normalized emittance, ε_N, due to the resulting excessive beam-beam tune shift.
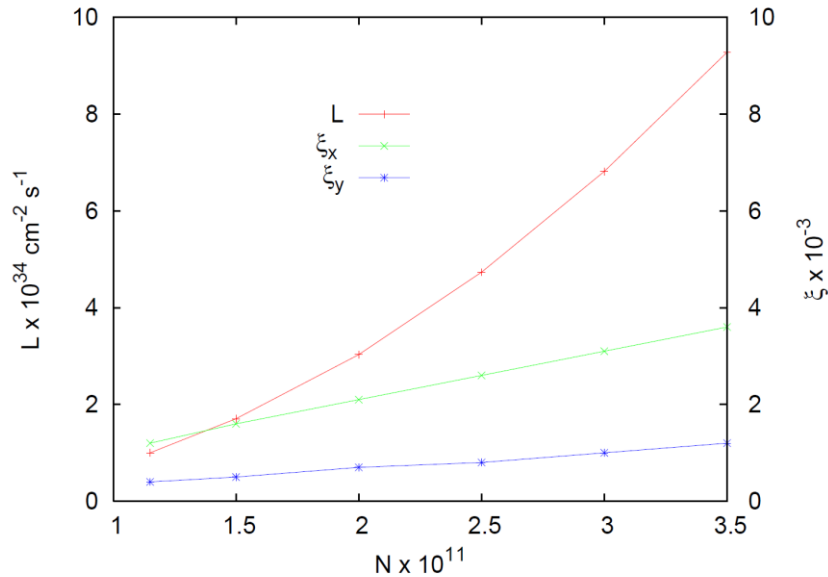

Figure 30: Luminosity and beam-beam tune shifts at one IP for ε_N=2.2 μm as a function of bunch population. For the luminosity calculation, the total number of bunches is 2808.

6.5.   MATCHING TO THE ARC

The LHC matching section is not flexible enough to match the highly perturbed β-functions to the values in the arc. The dispersion suppressor has, therefore, been used as well to match the IR optics to the arc, including the nonzero dispersion in the IR. The matching is done from a symmetric (IR) to an antisymmetric optics (LHC arc). Consequently, the matching sections from the IR to the arc left and right sides of the IP are asymmetric (Fig. 31).
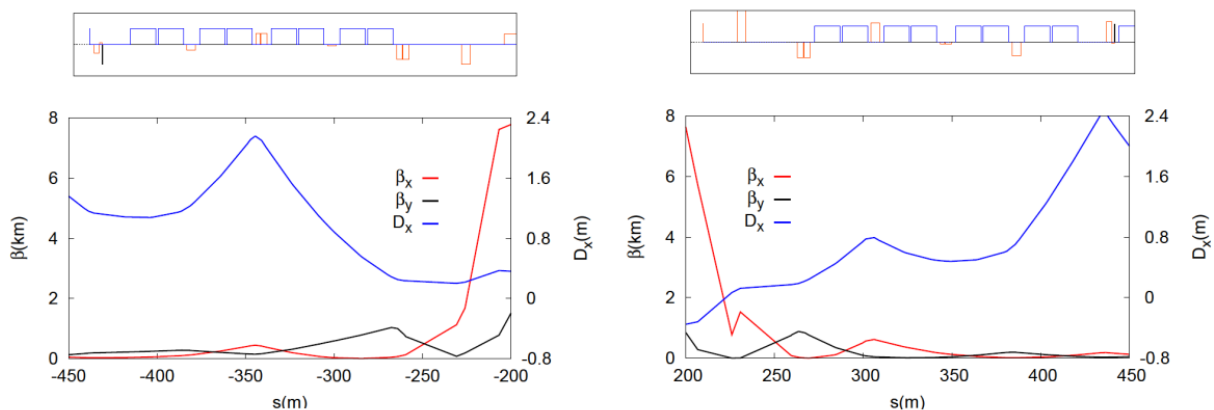

Figure 31: Matching section on the left (left) and right side (right) of IP1 for Beam 1.

We denote by L_{IR} and L_{ARC} the distances from the interaction point (IP) to the end of the IR and to the beginning of the arc, respectively. L_{IR} = 165 m, and L_{ARC} = 434. First, the matching is performed from a symmetric optics around the IP, over $\pm L_{IR}$, to an antisymmetric optics at location $\pm L_{ARC}$, which introduces different conditions one the two sides of the IP.

Second, the dispersion has a non-zero slope at the IP (implying dispersion across the IR), e.g. as a necessary ingredient for a local chromatic correction. Separator dipole magnets generate an antisymmetric dispersion. Therefore, the dispersion has different sign in $\pm L_{IR}$ while the dispersion in the arcs is positive at both sides. Two different MSs on each side of the IP also imply two different MSs for the two beams on one side of the IP. In order to obtain a more regular optics, a quasi-symmetric matching has been proposed by modifying one or several arc cells [Abe10].

6.5.1. Simplified matching

Figure 32 shows the arc optics for the first arc cell of the nominal LHC, for both beams.
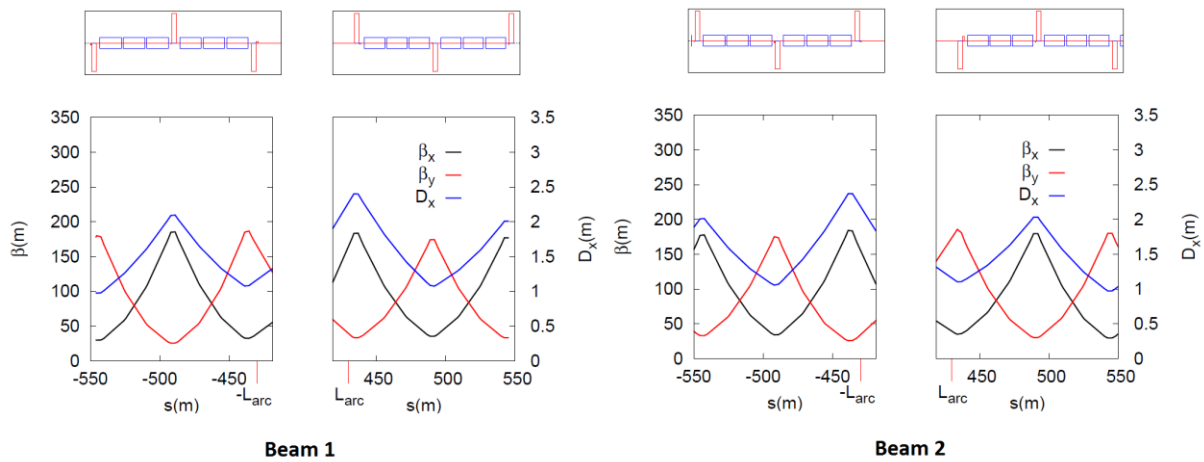

Figure 32: First arc cell on either side of IP1 in the nominal LHC for Beam 1 (left) and Beam 2 (right).

The results of varying only the existing weak "trim quadrupoles" of the first arc cell (MQTLI.11, MQT.12, MQT.13) to meet the conditions $\beta_x(L_{ARC}) = \beta_y(L_{ARC})$, $\alpha_x(L_{ARC}) = \alpha_y(L_{ARC})$, $\beta_x(-L_{ARC}) = \beta_y(-L_{ARC})$, $\alpha_x(-L_{ARC}) = \alpha_y(-L_{ARC})$, are plotted in Fig. 33. As $\beta_{x,y}(-L_{ARC}) \neq \beta_{x,y}(L_{ARC})$ and $\alpha_{x,y}(-L_{ARC}) \neq -\alpha_{x,y}(L_{ARC})$, we conclude that the trim quadrupoles do not give enough flexibility to "symmetrize" one arc cell, and that instead we need to individually power the main quadrupole magnets of the first arc cell (MQ.11, MQ.12 and MQ.13 at both sides), with results as shown in Fig. 34.
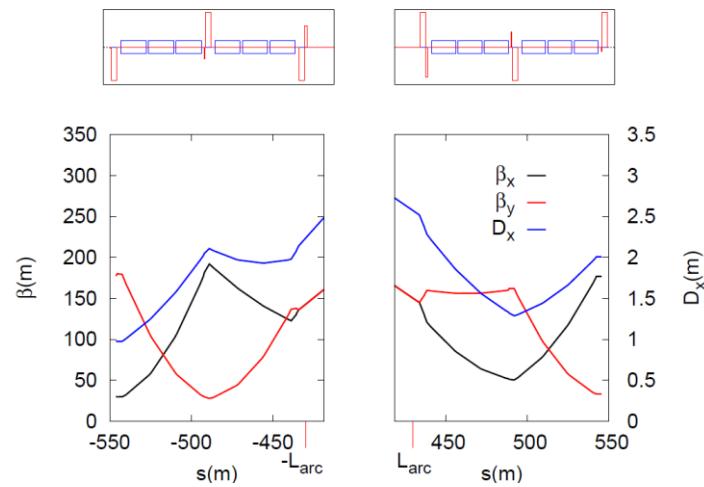
Figure 33: Modified optics of the first arc cell on each side of the IP (Beam 1), for matching to a symmetric IR optics using only the trim quadrupoles.
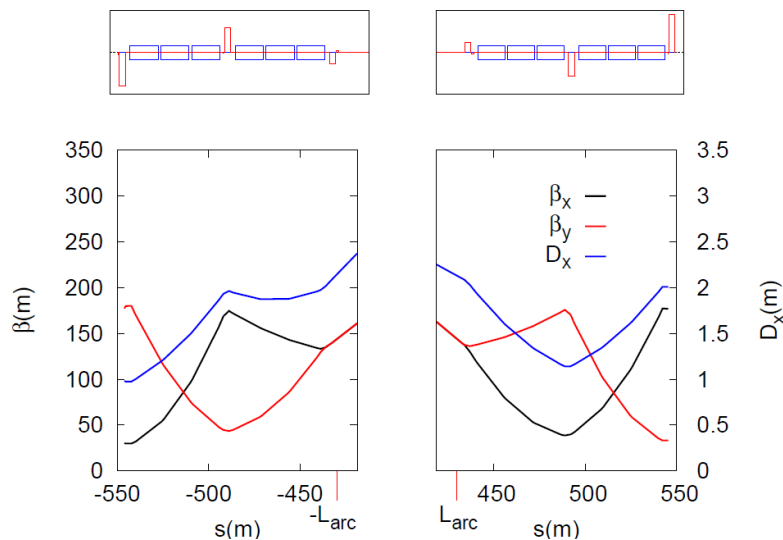

Figure 34: Modified optics of the first arc cell on each side of the IP (Beam 1), for matching to a symmetric IR optics using the main quadrupole magnets.

All the optical values are listed in Table 8. A last case corresponds to varying the main quadrupoles in the two last arc cells, (quadrupoles MQ.14 and MQ.15 in addition to those varied before). The corresponding optics is presented in Fig. 35.
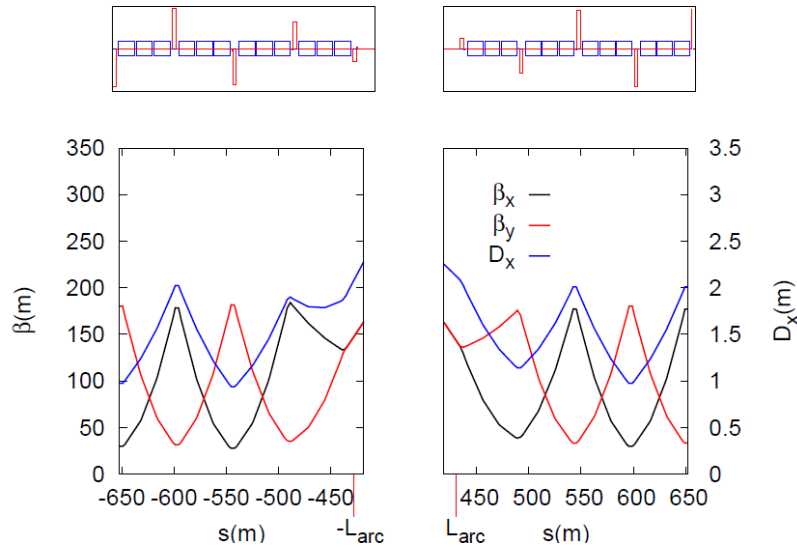
Figure 35: Modified optics of the first two arc cells on each side of the IP (Beam 1), for matching to a symmetric IR optics.

Table 8: Results of matching one or two arc cells to a symmetric IR optics.

	One modified arc cell by varying trim quads		One modified arc cell by varying main quads		Two modified arc cells by varying main quads	
	$-L_{ARC}$	L_{ARC}	$-L_{ARC}$	L_{ARC}	$-L_{ARC}$	L_{ARC}
$\beta_{x,y}$ [m]	136.2	145.1	137.5	137.5	137.5	137.5
$\alpha_{x,y}$	-0.71	0.60	- 0.68	0.74	- 0.74	0.74
D_x [m]	2.1	2.5	2.1	2.1	1.9	2.1
$D´_x$	0.02	-0.01	0.02	-0.01	0.02	-0.01

Anyway, it should be noted that it would be extremely expensive to power individually additional arc quads, due to their very high currents. The solution is to modify the cells and replace the MQ's by MQM's (but they will most likely be longer).

6.6. COMPENSATION OF GEOMETRIC ABERRATIONS

The higher order terms of the DHQ must be compensated. A sextupole spaced at $\Delta\mu_x=\pi$, $\Delta\mu_y=\pi$ from the DHQ can compensate the geometric aberrations if its sextupole strength fulfills the relation $k_{s2}=(\beta_y/\beta_x)^{1/2}k_{s1}$. Figure 36 shows the beam sizes as a function of the order considered, as computed with MAPCLASS, for a monochromatic beam and for a Gaussian energy distribution with $\sigma_\delta=1.4\times10^{-4}$, as for the present LHC. This analysis is considering only a single pass through (half of) the final-focus system.
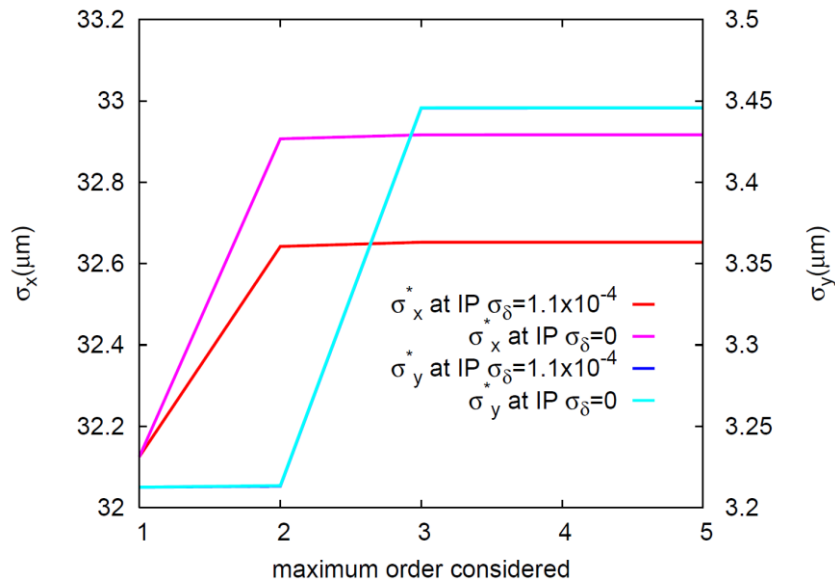
Figure 36: MAPCLASS analysis of beam size versus aberration order

Even though the aberrations look reasonably compensated, this is a necessary condition but by far not sufficient. Indeed multi-turn tracking simulations reveal that the aberrations are still not sufficiently compensated. For a perfect compensation of the aberrations, between two thick sextupolar elements the β ratio β_y/β_x, should be the same along the length of the elements and the variation of the phase advances between the elements should be as small as possible. Figure 37 demonstrates that neither of these two conditions is fulfilled. The β ratio varies from 98 to 30 and there is a significant phase-advance variation.
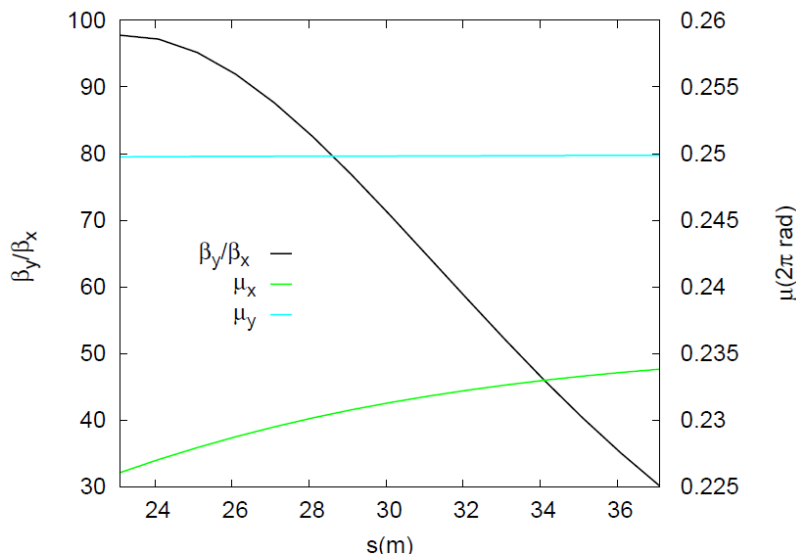

Figure 37: β-ratio and phase advance between the DHQ and its compensating sextupole.

In principle this is option would be excluded as a possible solution. The reason is the length of the DHQ. A solution could be found if the vertical final focus is made from a DHQ and quadrupoles, as sketched in Fig. 38. The DHQ would help separate the beams thanks to the dipolar field, and perform part of the focusing. Following this, bending magnets could be installed to help bring the beams to an optimum separation so that they could pass through

different channels of an upstream quadrupole with much higher quadrupolar field. In order to explore the potential performance of such approach, the sextupolar field has been concentrated as a thin lens element located in the center of the DHQ but maintaining the same integrated sextupolar strength, as the worst case scenario. A place was found with a perfect phase transformation of $\Delta\mu_x=\pi$, $\Delta\mu_y=\pi$, and with the same factor β_x/β_y at the location of the DHQ and the compensating sextupole. First tracking simulations with on-energy particles showed no dynamic-aperture reduction with respect to the nominal LHC. This indicates the good correction of the geometric aberrations. Figures 38 and 39 present the off-momentum beta-beat for an energy offset of $3\sigma_E$. This might reflect the effect of the local chromatic correction, that takes place in the horizontal plane only.
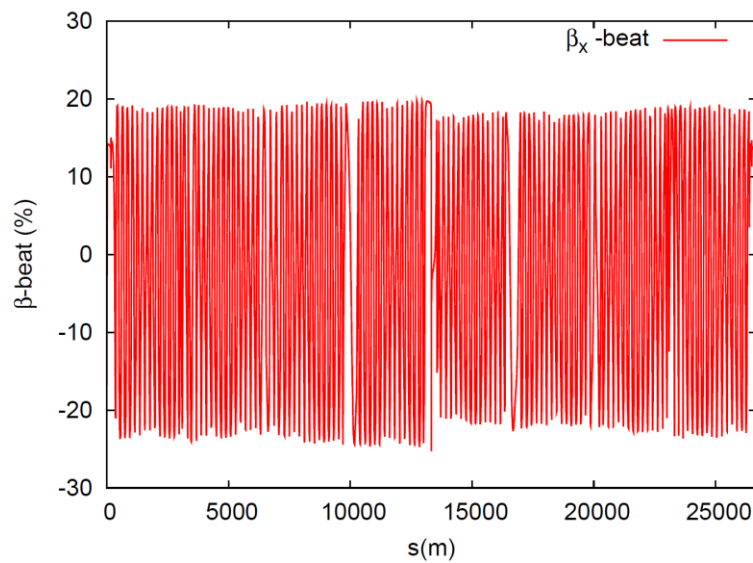

Figure 38: horizontal β-beating for an energy offset of $3\sigma_E$
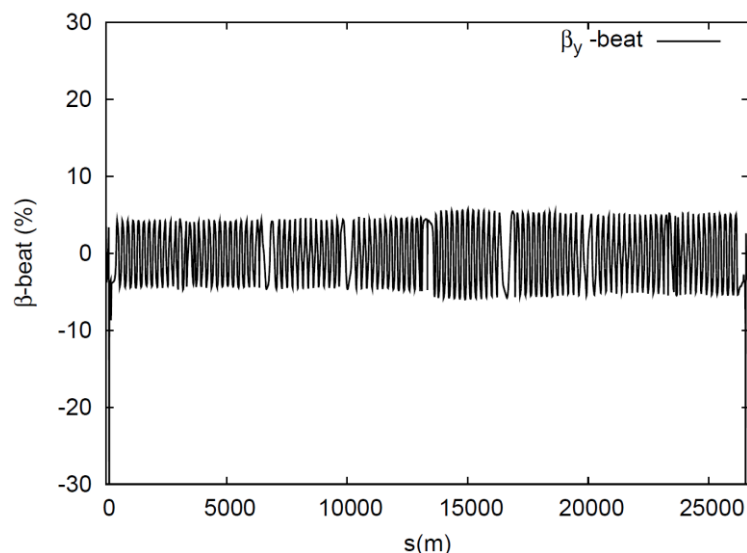

Figure 39: vertical β-beating for an energy offset of $3\sigma_E$

Next, tracking simulations were performed for off-energy particles ($3\sigma_E$). The resulting survival plots are shown in Figs. 40 and 41.
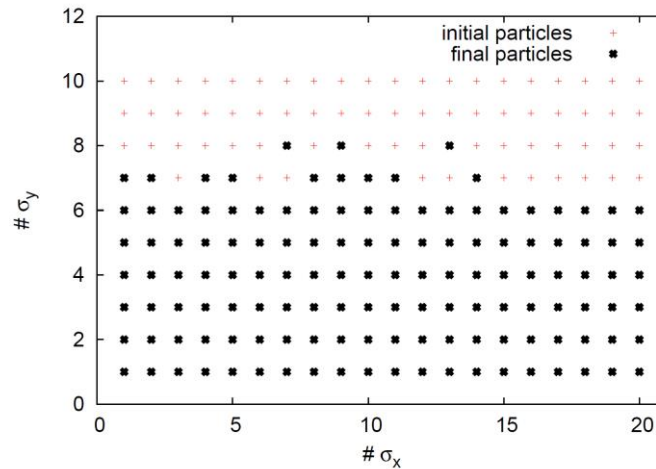
Figure 40: Survival plot for 10^3 turns at an energy offset of $3\sigma_E$
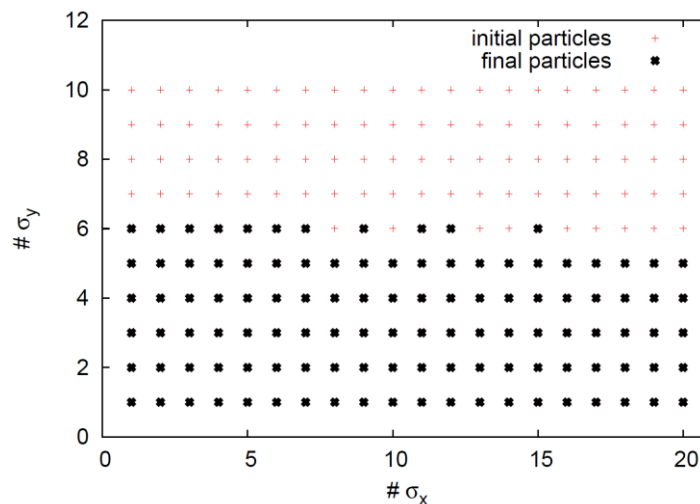

Figure 41: Survival plot for 10^4 turns at an energy offset of $3\sigma_E$.

Clearly, the dynamic aperture is limited in the vertical plane. This could be caused either by the breakdown of the phase relations between the two sextupolar components – namely between the DHQ and the compensating sextupole, or it could be related to second order dispersion.

6.7. SUBSTITUTING DHQ BY DHQ+QUAD

An important limitation arises from the fact that the ratio between the sextupolar and the quadrupolar strengths in the DHQ is very high. A long element must be placed to focus the vertical β–function. Due to the long length, the high order terms from the intrinsic sextupole components are difficult to compensate due to a number of reasons:

- the integrated sextupolar strength is high
- the phase advance along the quadrupole is along
- the ratio β_y/β_x changes along the element

These effects are mitigated by splitting the final quadrupole into a shorter DHQ (with sextupole and quadrupole components) and a subsequent pure quadrupole, with intermediate bending, as sketched in Fig. 42.
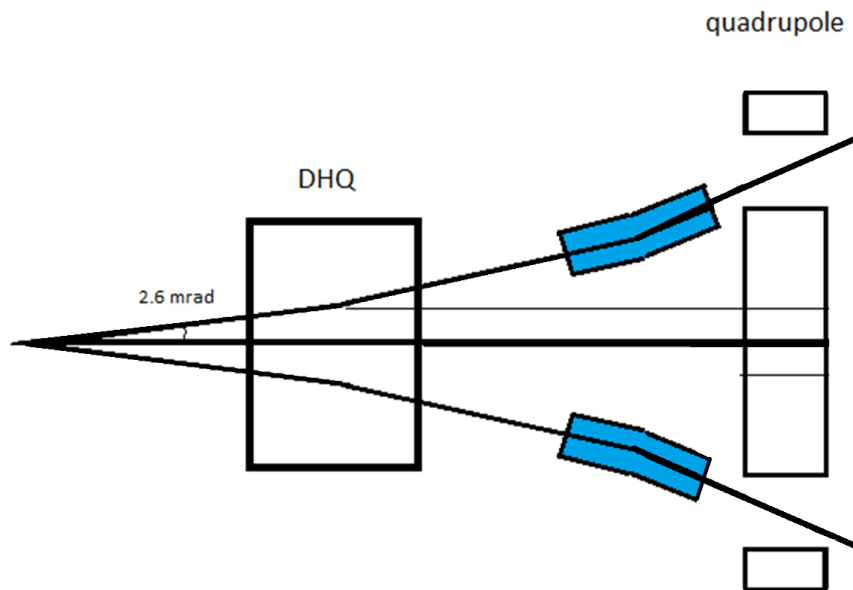
Figure 42: Sketch of a final element split into DHQ and superconducting quadrupole.

7.   AN INTERACTION REGION FOR HE-LHC

7.1.   PARAMETERS

A similar idea of using flat beam collisions with LPA was proposed for the HE-LHC [18] with a beam energy of 16.5 TeV. The very low emittances due to larger relativistic gamma lead to even smaller maximum tune shifts than for the cr-w LHC, as a consequence of the increased Piwinski angle with lower horizontal beam size. Also, the short synchrotron damping times allow operation witn unequal transverse emittances, i.e. truly flat beams. Two possible parameter sets are listed in Table 8.

An interesting case is obtained if the HE-LHC is realized as a proton antiproton collider. In that case, a quadrupole with common aperture, as one of the present LHC triplet, can be used as final quadrupole and provide a symmetric optics, thanks to the fact that the charge have opposite sign for the two beams.

Table 9: Flat beam parameters for HE-LHC.

	θ = 2 mrad	θ = 8 mrad
initial luminosity [cm^{-2} s^{-1}]	2.3x10^{34}	2x10^3
N$_0$ [10^{11}]	2.45	3.05
Crossing angle [mrad]	2	8
Technology for last quad.	Double-half quad.	Double aperture quad.
IP beta function (H/V) [m]	3/0.03	
Norm. initial emittance (H/V) [μm rad]	2.1	
Initial beam size IP [μm]	19/1.9	
Number of bunches	1404	
Crossing scheme	horizontal at the two IP	
Initial Piwinski angle	4.1	16.3
Initial total tune shifts [10^{-3}]	3.2/1.3	0.3/0.4
maximum total tune shifts	8.9/2.4	1.1/1.2
Beam separation [σ]	317	12680
Long. SR emittance damping time [h]	1.01	
Transverse SR emittance damping time [h]	2.02	
Initial horizontal IBS emittance rise time [h]	37.51	21.1
Initial vertical IBS emittance rise time [h]	72.02	42.2
Initial longitudinal IBS rise time [h]	72.45	40.7
Beam intensity lifetime [h]	14.6	29.9
Optimum run time [h]	6	8.5
Opt. av. Int. luminosity/day [fb-1]	1.63	1.93

7.2. TIME EVOLUTION

The time evolution of luminosity, emittances, tune shifts, beam sizes, transverse beam-size ratio, bunch length and Piwinski angle for either of the two flat-beam HE-LHC scenarios was computed by O. Dominguez (EPFL-CERN), with results presented in Figs. 39-45 for a crossing angle of 2 mrad or 8 mrad, respectively. During a run, the number of particles decreases as a consequence of the burn-off. Due to the short SR damping times, there can also be a significant decrease in transverse emittance. With low Piwinski angle, such as for the standard HE-LHC with round beams and small crossing angle, the limitation in the beam-beam tune shift obliges one to apply a continuous controlled external excitation in the longitudinal as well as in the two transverse planes. However, with a large Piwinski angle and flat beams, the tune shifts are much smaller and the need for controlled blow up is eliminated. The parameters can be adjusted so as to use the radiation damping, together with the natural excitation from intrabeam scattering, to compensate for the effect of the burn off.
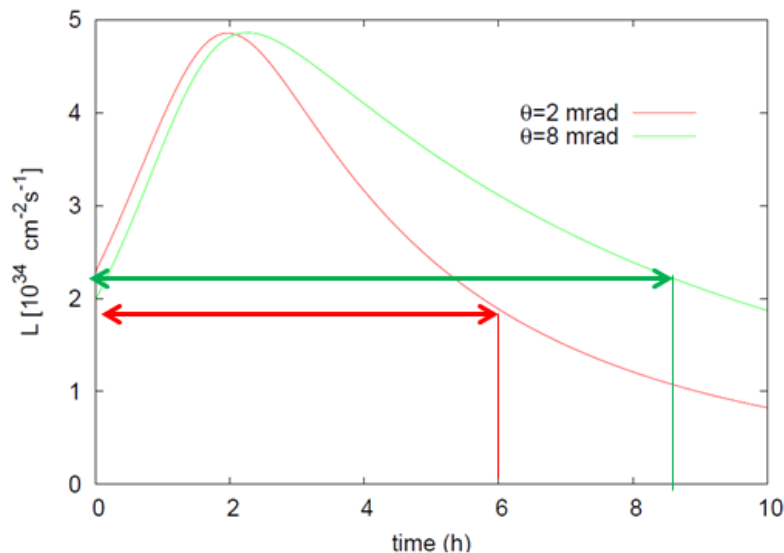

Figure 43: Luminosity time evolution for the HE-LHC scenarios

7.2.1. Time evolution for θ=2 mrad
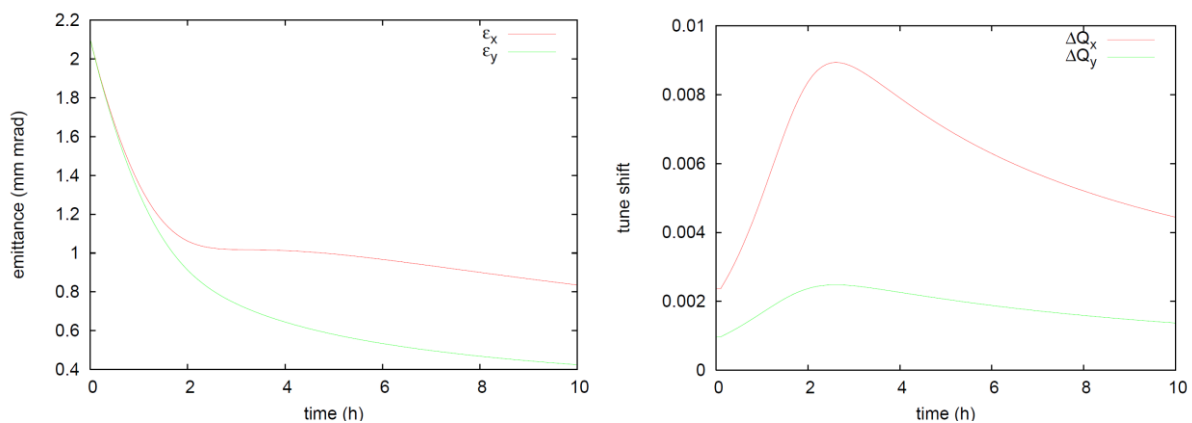

Figure 44: Time evolution of emittance (left) and total tune shifts (right) for θ=2 mrad.

Figure45: Time evolution of beam size ratio (left) and transverse beam sizes (right) for θ=2 mrad.

Figure 46: Time evolution of rms bunch length (left) and Piwinski angle (right) for θ=2 mrad.

7.2.2. Time evolution for θ=8 mrad

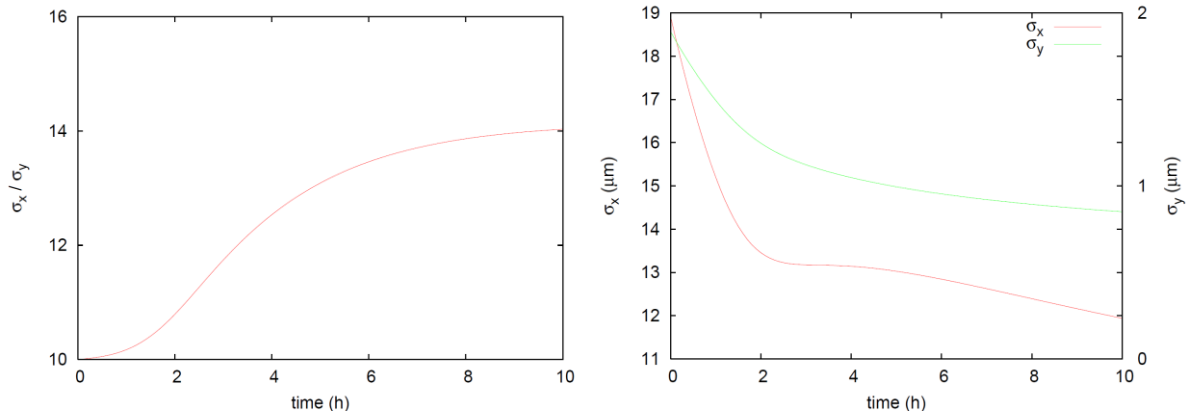*Figure 47: Time evolution of emittance (left) and total tune shifts (right) for θ=8 mrad.*

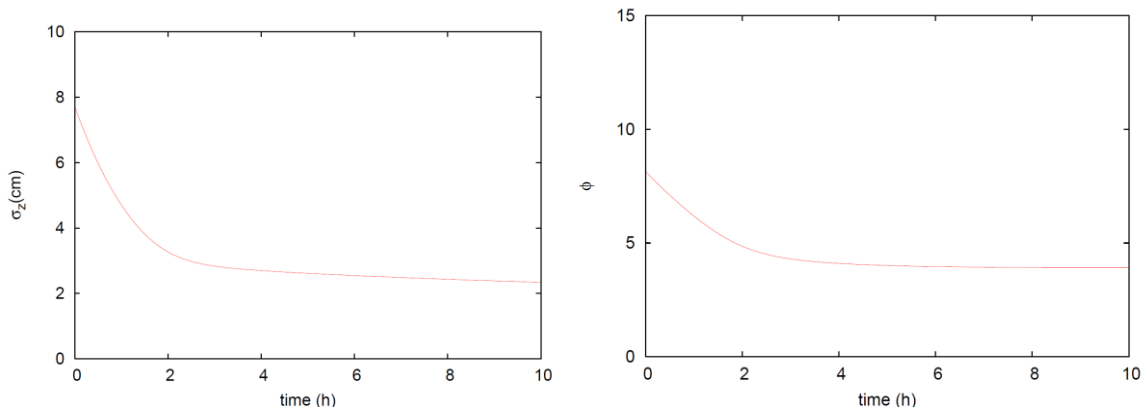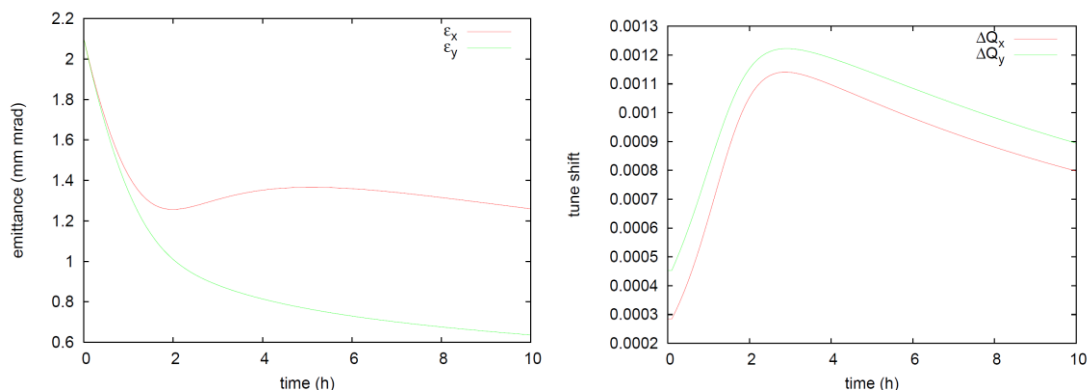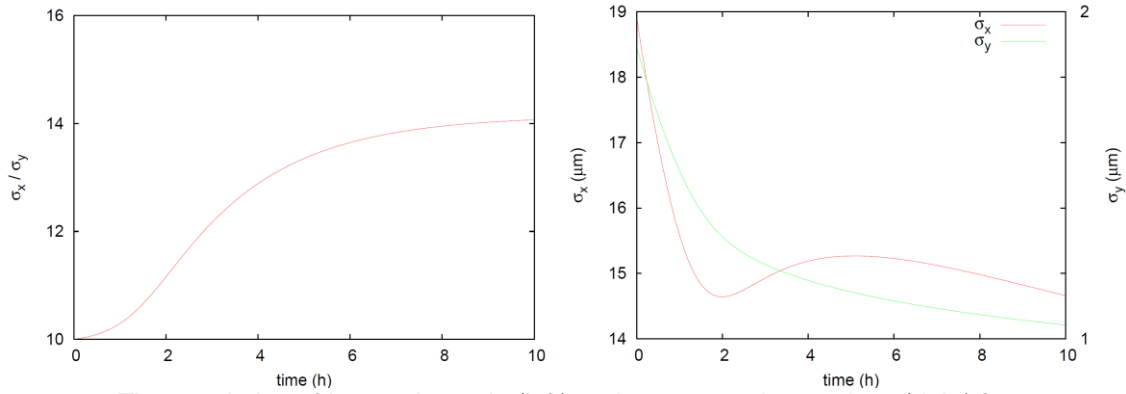*Figure 48: Time evolution of beam size ratio (left) and transverse beam sizes (right) for ϴ=2 mrad.*

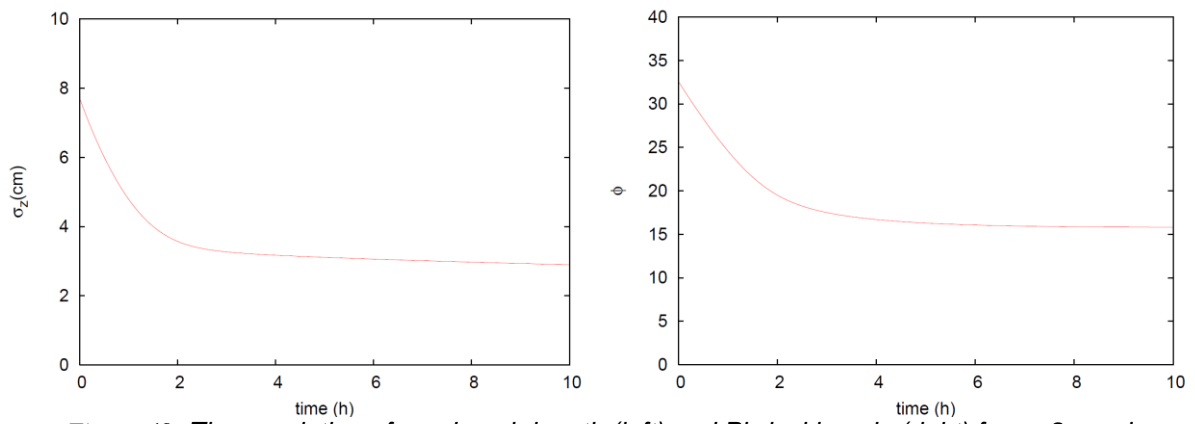*Figure 49: Time evolution of rms bunch length (left) and Piwinski angle (right) for ϴ=8 mrad.*

8. CONCLUSIONS

We have developed an elegant conceptual optics solution for a future LHC luminosity upgrade, combining flat beams, local chromatic correction, large Piwinski angle and the option of crab-waist collisions. The scheme requires a non-zero slope of dispersion at the IP and a new single-aperture final focusing element, which combines dipole and sextupolar field components. The quadrupole feed down field focuses both beams in the vertical plane. The sextupole component together with the non-zero dispersion is used to correct the chromaticity locally. Orbit, dispersion and beta functions were matched to the existing LHC arcs. Dynamic aperture is still a concern. The geometric aberrations could be corrected perfectly by a second sextupole if the magnets were short. However the double half quadrupole is quite long, which introduces intrinsic octupolar aberrations in addition to rendering difficult the compensation with a second sextupole. A segmentation of the final quadrupole, to confine the sextupole field to a shorter region, is proposed as mitigation (Fig. 42). A similar final focus system, for a single beam was designed and qualified for the LHeC. Possible merits of, and parameters for, applying the described approach at the HE-LHC have also been investigated. Successful beam experiments testing key concepts, like crab-waist, large Piwinski angle and flat beams, were conducted, analysed and prepared at DAΦNE and at the LHC, respectively.

9. BIBLIOGRAPHY

1.	F. Ruggiero, F. Zimmermann, Luminosity Optimization Near the Beam-Beam Limit by Increasing Bunch Length or Crossing Angle, Phys. Rev. ST Accel. Beams 5, 061001 (2002).
2.	P. Raimondi, 2nd SuperB Workshop, Frascati 2006.
3.	M. Zobov, DAΦNE Operating Experience with Crab Waist Collisions, RuPAC2008, Zvenigorod, arXiv:0810.2211v1.
4.	S. Fartoukh, "An Achromatic Telescopic Squeezing (ATS) Scheme for LHC Upgrade", Proc. IPAC'11 San Sebastián, Spain, p. 2088
5.	P.Raimondi, A Novel final focus design for high-energy linear colliders, Proc. EPAC'2000 Vienna (2000).
6.	P. Raimondi and A. Seryi, A Novel final focus design for future linear colliders, Phys. Rev. Lett. 86, 3779, 2001.
7.	C.J. Johnstone, Local chromatic correction of the LHC, Proc. PAC97 Vancouver, 1997.
8.	R. de Maria, O.S. Bruning, P. Raimondi, LHC IR upgrade: a dipole first option with local chromaticity correction, Proc. 10th European Conference, EPAC 2006, Edinburgh, UK, June 26-30, 2006.
9.	A. Faus-Golfe et al, Limits on Chromaticity Correction, in Proc. LHC LUMI 2006 CARE-HHH-APD Workshop, 16-0 October 2006, Valencia, CERN-2007-002.
10.	S. Fartoukh, "An Achromatic Telescopic Squeezing (ATS) Scheme for LHC Upgrade", Proc. IPAC'11 San Sebastián, Spain, p. 2088.
11.	K. Ohmi and K. Oide, Chaos and Emittance Growth due to Nonlinear Interactions in a Circular Accelerator," Phys. Rev. ST Accel. Beams 10, 014401 (2007).
12.	K. Ohmi, Study of beam-beam interaction with a large Piwinski angle at LHC, in Proc. CARE-HHH-APD workshop BEAM'07, 1–5 October 2007, CERN, Geneva, CERN YellowReport CERN-2008-005 (2008).
13.	P. Raimondi, D. Shatilov, M. Zobov, Beam-beam issues for colliding schemes with large Piwinski angle and crabbed waist, LNF-07-003-IR, physics/0702033 (2007).
14.	J. Laskar, Icarus 88, 266 (1990).
15.	S. Russenschuck, Field Computation for Accelerator Magnets, Wiley-VCH 2010
16.	K. Kanazawa et al, NIMA 499 (2003) 7599
17.	S. Fartoukh, A semi-analytical method to generate an arbitrary 2D magnetic field and determine the associated current distribution, LHC Project Report 1012 (2007)
18.	E. Todesco, F. Zimmermann (eds.), Proc.EuCARD-AccNet-EuroLumi Workshop: The High-Energy Large Hadron Collider, Malta, Oct. 2010, CERN-2001-003
19.	A. Faus-Golfe. "Looking for a symmetric LHC low-beta insertion," LHC note 336, 1995.

10. PUBLICATIONS

Shat01	D. Shatilov, et al, Application of frequency map analysis to beam-beam effects study in crab waist collision scheme. PRST-AB 14:014001 (2011).
Abe01	J.L. Abelleira,et al, "Design Status of LHeC Linac-Ring Interaction Region", *Proc. of the 2011 International Particle Accelerator Conference, San Sebastian, Spain,* p. 2796 (2011).
Abe02	J.L. Abelleira et al, "Final-Focus Optics for the LHeC Electron Beam Line", *Proc. of the 2012 International Particle Accelerator Conference, New Orleans,USA,* p. 1861 (2012).
Abe03	The LHeC study group, J L Abelleira *et al* 2012 *J. Phys. G: Nucl. Part. Phys.* 39 075001.
Abe04	J.L. Abelleira, "LHeC Final Focus System", contribution to *2012 CERN-ECFA-NuPECC Workshop on the LHeC, 14-15 June 2012, Chavannes-de-Bogis, Switzerland.*
Abe05	J.L. Abelleira et al. CERN-ATS-Note-2012-091. MD Large Piwinski angle
Abe06	J.L. Abelleira,"Towards an extremely-flat beam optics with large crossing angle for the LHC", contribution to EUCARD Annual Meeting, April 25-27, 2012, Warsaw, Poland.
Abe07	J.L. Abelleira et al, "Local Chromatic Correction Scheme and Crab-Waist Collisions for an Ultra-Low Beta* at the LHC ", Proc. IPAC'12 New Orleans, U.S.A. p.118.
Abe08	J.L. Abelleira, "Flat beam IR optics", contribution to joint EuCARD-HiLumi-Snowmass Workshop on "Frontier Capabilities for Hadron Colliders." February 22-23; 2013, CERN, Switzerland.
Abe09	J.L. Abelleira et al, "LHC Optics with Crab-Waist Collisions and Local Chromatic Correction". Proc. IPAC'13 Shanghai, China.
Abe10	J.L. Abelleira et al, "Matching Antisymmetric Arc Optics to Symmetric Interaction Region", Proc. IPAC'13 Shanghai, China.

11. FUTURE PLANS

Future work needs to improve the dynamic aperture. A promising approach is the proposed splitting of the DHQ into two components. The detailed reason for the dynamic-aperture limitation in the vertical plane also deserves further studies.

An optics design for the flat-beam scenarios of HE-LHC/VHE-LHC should be developed. It is likely that such optics will become the first realistic application of the scheme presented in this report.

An experiment with quasi-flat beams was prepared for the 2012 LHC run. It should be executed after resuming LHC beam operation in 2015.

This work has demonstrated the possibility, in principle, to design an IR for the LHC or for future hadron colliders using similar concepts and characteristics as the latest schemes developed for increasing the luminosity at lepton factories, such as the Φ-Factory DAΦNE in operation at LNF and the planned SuperKEKB B-factory in Japan.

ANNEX: GLOSSARY

Acronym	Definition
L*	Distance between the last element and the IP in an accelerator lattice
DHQ	Double-half quadrupole
IP	Interaction point
ROXIE	Software created by Stephan Russenschuck at CERN for the electromagnetic simulation and optimization of accelerator magnets.
SR	Synchrotron radiation.
$\sigma_{x,y,s}*$	Beam size in the IP in an accelerator lattice for the horizontal, vertical and longitudinal planes, respectively
θ_c	Crossing angle between the beams at collision.
β	Amplitude optical function.
CP	Collision point
LPA	Large Piwinski Angle. Usually considered when the Piwinski angle Φ is bigger than 1.
CR-W	Crab-waist scheme.
Δin	Inner normalized separation. Separation between two colliding beams in units of beam size in the plane of crossing.
MS	Matching section
MD	Machine development in the LHC.
MAPCLASS	Code written by Rogelio Tomas (CERN) to analytically track particle beams. **R. Tomas, CERN AB-Note-2006-017 (ABP) (2006).**